



GCM-related uncertainty for river flows and inundation under climate change: the Inner Niger Delta

Julian R. Thompson, Andrew Crawley & Daniel G. Kingston

To cite this article: Julian R. Thompson, Andrew Crawley & Daniel G. Kingston (2015): GCM-related uncertainty for river flows and inundation under climate change: the Inner Niger Delta, Hydrological Sciences Journal, DOI: [10.1080/02626667.2015.1117173](https://doi.org/10.1080/02626667.2015.1117173)

To link to this article: <http://dx.doi.org/10.1080/02626667.2015.1117173>



Copyright © 2015 The Author(s). Published by Taylor & Francis.



Accepted author version posted online: 16 Dec 2015.
Published online: 16 Dec 2015.



Submit your article to this journal [↗](#)



Article views: 174



View related articles [↗](#)



View Crossmark data [↗](#)

Publisher: Taylor & Francis & IAHS

Journal: *Hydrological Sciences Journal*

DOI: 10.1080/02626667.2015.1117173

GCM-related uncertainty for river flows and inundation under climate change: The Inner Niger Delta

Julian R. Thompson¹, Andrew Crawley¹, Daniel G. Kingston²

1. *Wetland Research Unit, UCL Department of Geography, University College London, Gower Street London, WC1E 6BT, UK.*

2. *Department of Geography, University of Otago, PO Box 56, Dunedin, New Zealand.*

Email: j.r.thompson@ucl.ac.uk

Abstract: A semi-distributed hydrological model of the Niger River above and including the Inner Delta is developed. GCM-related uncertainty in climate change impacts are investigated using seven GCMs for a 2 °C increase in global mean temperature, the hypothesised threshold of 'dangerous' climate change. Declines in precipitation predominate, although some GCMs project increases for some sub-catchments, whilst PET increases for all scenarios. Inter-GCM uncertainty in projected precipitation is three to five times that of PET. With the exception of one GCM (HadGEM1), which projects a very small increase (3.9%), river inflows to the Delta decline. There is considerable uncertainty in the magnitude of these reductions, ranging from 0.8% (HadCM3) to 52.7% (IPSL). Whilst flood extent for HadGEM1 increases (mean annual peak +1405 km² / +10.2%), for other GCMs it declines. These declines range from almost negligible changes to a 7903 km² (57.3%) reduction in the mean annual peak.

Key words: Inner Niger Delta; climate change; uncertainty; hydrological modelling

INTRODUCTION

Climate change is likely to exert a major influence upon wetlands with many impacts being driven by hydrological changes (Ramsar Bureau 2002, Acreman *et al.* 2009). Intensification of the global hydrological cycle is projected to have major implications for catchment hydrological processes (e.g. Kundzewicz *et al.* 2007, Bates *et al.* 2007). These impacts, which are projected to vary from region to region (Arnell and Gosling 2013), may in turn modify the magnitude and temporal distribution of flows of water into and out of wetlands and consequently wetland hydrological regimes (Baker *et al.* 2009, Erwin 2009). Changing spatial and temporal patterns in water levels and flood extent may alter the ecological character of wetlands and the ecosystem services they provide (Erwin 2009, Thompson *et al.* 2009).

There is, however, considerable uncertainty in the impacts of climate change on hydrological systems including wetlands. Impacts are commonly projected by driving a hydrological model that has been calibrated for a baseline period with climate projections derived by forcing General Circulation Models (GCMs) with greenhouse gas emissions scenarios. Hydrological changes can then be used to infer impacts on, for example, ecological conditions or ecosystem service provision (e.g. Thompson *et al.* 2009, Singh *et al.* 2010, 2011, Thompson *et al.* 2014b). Each stage of climate change impact assessments introduces uncertainty (Gosling *et al.* 2011). There is uncertainty in the emissions scenarios whilst alternative process representations and parameterisation schemes cause different GCMs to produce different projections for the same emissions scenario. Downscaling of GCM projections to finer spatial and temporal scales for hydrological modelling introduces further uncertainty. Hydrological models are subject to a range of uncertainties that include imprecise knowledge of hydrological system behaviour, which may include inadequate information on water resource management influences, as well incomplete or erroneous hydrometric data (e.g. Van Dijk *et al.* 2008). Different hydrological models of an

individual river basin that produce acceptable results for a baseline period may respond differently when forced with the same climate change scenario (Chiew *et al.* 2008, Gosling and Arnell 2011, Haddeland *et al.* 2011, Thompson *et al.* 2013). Assessment of the impacts of projected hydrological changes upon wetlands is uncertain due to imprecise understanding of the relationships between wetland hydrology, hydrochemistry and ecology. This includes limited knowledge of the water level requirements of individual wetland species and communities as well as the hydrological controls upon ecosystem service provision. Further uncertainty is associated with future water management responses to climate change (Van Dijk *et al.* 2008) that may in turn induce hydrological modifications. Of these different sources of uncertainty, GCM-related uncertainty has frequently been found to be the most significant (e.g. Graham *et al.* 2007, Prudhomme and Davies 2009), although other factors may not be negligible (Haddeland *et al.* 2011, Thompson *et al.* 2013). Indeed, assessments of uncertainty related to the translation of hydrological changes to ecological impacts are very limited.

GCM-related uncertainty for river flow for a series of catchments around the world including examples in North (Thorne 2011) and South America (Nóbrega *et al.* 2011), Africa (Hughes *et al.* 2011) and Asia (e.g. Kingston *et al.* 2011) was assessed using a consistent set of climate change scenarios and catchment hydrological models as part of the QUEST-GSI project. This integrated, multi-sector and multi-scale analysis of climate change impacts employed unified climate drivers to enable a consistent analysis of impacts, associated uncertainty and vulnerability (Todd *et al.* 2011, <http://www.met.reading.ac.uk/research/quest-gsi/>). The dominance of GCM-related uncertainty was clearly demonstrated by the QUEST-GSI catchment modelling studies (Gosling *et al.* 2011). Only one study explicitly assessed inter-GCM uncertainty on wetland hydrology, in this case Loktak Lake, an internationally important lacustrine wetland in northeast India (Singh *et al.* 2010). The current study employs the same scenarios to investigate GCM-related uncertainty for one of Africa's largest wetlands, the Inner Niger Delta, and the catchment that supports it.

DATA AND METHODS

The Upper Niger and the Inner Niger Delta

Mali's Inner Niger Delta is one of West Africa's largest floodplain wetlands. It is located at the downstream end of the 147 000 km² Upper Niger catchment, which has its headwaters in the Fouta Djallon highlands of Guinea, and the Bani (129 000 km²), a major tributary of the Niger that rises in the Ivory Coast (Figure 1, Zwarts *et al.* 2005a).

The Inter-Tropical Convergence Zone, the region where the northern and southern hemisphere trade winds converge and which is associated with abundant precipitation, exerts a dominant influence upon the hydrology of the Delta and its catchment, similar to other African floodplains (e.g. Thompson 1996). Rainfall exhibits large inter-annual variability. Mean annual rainfall (derived for 1950–2000 from the CRU TS 3.0 dataset – see below) over the headwaters of the Niger exceeds 2100 mm whilst over upstream parts of the Bani it is around 1500 mm. In contrast, over the downstream end of the Delta, annual rainfall is on average close to 250 mm. The southwest–northeast rainfall gradient is accompanied by a decline in wet season duration from eight months (March–October) in the southwest to three months (July–September) over the Delta. Annual peak rainfall occurs in August and the intervening dry period is associated with little or no rainfall. Potential evapotranspiration (PET; based on the Hargreaves method and CRU TS 3.0 data – see below) also shows a southwest–northeast gradient but the direction is reversed to that of rainfall. Mean annual PET in the southwest approaches 1800 mm and over the Delta it is around 2150 mm.

River flow exhibits large intra-annual variability. In common with rivers throughout West Africa (e.g. Drijver and Marchand 1985, Adams 1992) dry season flows are small in comparison to wet season peaks. Above the Delta the lowest discharges occur during the period March–May. River flows begin to rise rapidly with the onset of the rains and the annual peak occurs in

September (Zwarts *et al.* 2005a). Discharges decline thereafter, albeit at a slightly slower rate than the rise at the start of the wet season.

The seasonal river flow results in similar intra-annual variability in flood extent within the Delta. Lowest water levels occur between May and July and the area of permanent water coverage is less than 4000 km² and very small in particularly dry years (Sutcliffe and Parks 1989, Zwarts and Grigoras 2005). Peak flooding, which is most often achieved in November, is often stated as reaching 30 000 km² (Grove, 1985, Sutcliffe and Parks 1989). However, it varies substantially from year to year. Zwarts and Grigoras (2005) identified a range from over 24 000 km² in the 1950s to less than 8000 km² at the height of the 1980s drought.

The Delta exerts an important influence upon downstream river flows. Evaporation from inundated areas removes large volumes of water whilst further losses can be attributed to seepage beneath these areas (Beadle 1974, Zwarts *et al.* 2005a). On average around 55% of the combined inflows to the Delta at Ke-Macina and Beney-Kegny reaches Douna although the magnitude of losses increases with flood level due to larger inundation extents (Zwarts and Grigoras 2005, Zwarts *et al.* 2005a). The passage of the annual peak through the Delta takes 3–4 months so that at Dire the highest flows occur in November or December (John *et al.*, 1993; Sutcliffe and Parks, 1989) whilst the duration of the high flow period extends from 2–3 months upstream to 7 months downstream (Zwarts *et al.* 2005a).

The Inner Niger Delta is extremely productive, especially compared to the surrounding drylands. It is central to the livelihoods of over 1 million people (Zwarts and Kone 2005a), supporting agriculture, especially rice cultivation, fishing and grazing of cows, sheep and goats. In common with other African floodplains (e.g. Thompson and Polet 1998), productivity is linked to the annual flood (Goosen and Kone 2005, Zwarts and Diallo 2005, Zwarts and Kone 2005b), with vegetation zonation being controlled by water depth and its seasonal variation (Zwarts *et al.* 2005b). Fish recruitment and survival through the dry season is related to the previous peak flood level and duration of flooding (e.g. Welcomme 1986, Zwarts and Diallo 2005). The Delta is also a biological hotspot, and is one of the world's largest Ramsar sites (van der Kamp *et al.* 2005).

Changes to flooding within the Delta can be expected due to two factors. The first is upstream water resource schemes. Whilst the Sotuba hydropower dam (constructed in 1929) on the Niger just below Bamako has limited hydrological impacts due to its small reservoir, the larger Sélingué Dam (1982) on the Sakarani River (Figure 1) reduces peak Niger flows at Ke-Macina by 10–20% in wet years and 20–30% in dry years (Zwarts *et al.*, 2005a). Dry season releases double the modest natural flows. The Markala Barrage (constructed between 1937 and 1945) diverts water to irrigate the Office du Niger project (currently 740 km², a small fraction of the planned 9600 km²). These diversions are equivalent to only a few percent of wet season flows but during the dry season irrigation diversions can cut river flow by over half (Zwarts *et al.* 2005a). The impacts of the Talo Dam on the Bani, which was constructed in 2006 and is designed for irrigation, are at present difficult to gauge. Plans for future dams include the Fomi hydropower dam (above Kankan on the Niandan tributary) that is currently being seriously considered and another dam on the Bani (Zwarts *et al.* 2005a). Climate change-related alterations to precipitation and evapotranspiration are also likely to impact river flows and flooding within the Inner Delta. Establishing the nature, magnitude and the degree of uncertainty of climate change-related modifications to river flow and flooding is the aim of the current study.

Hydrological modelling

A semi-distributed, conceptual hydrological model operating at a monthly time step was developed for the Niger catchment upstream of the Inner Niger Delta. It also incorporated an element simulating inundation within the Delta. Model simulations covered the period 1950–2000 (calibration: 1950–1975, validation: 1976–2000, baseline for climate change scenarios: 1961–1990 – discussed below). The model was implemented using the STELLA systems modelling software (Version 10, isee systems) which provides a high level visual-oriented software and simulation

language and has been employed in a number of catchment and wetland hydrological modelling studies (e.g. Voinov *et al.* 2007, Zhang and Mitsch 2005, Ho *et al.* 2015).

Separate sub-models, each with an identical structure, were developed for 11 sub-catchments defined by the location of a gauging station at their downstream outlet (Figure 1). The area draining to each gauging station was established using the USGS GTOPO30 digital elevation model (30-arc second or approximately 1 km resolution) and the ArcGIS 10 (Esri) ‘Hydrology’ geoprocessing tools. In a similar approach to that adopted by Ho *et al.* (2015), each sub-catchment model comprised three reservoirs representing the soil, groundwater and channel (i.e. surface water) stores (SS, GWS and CS, respectively) for which the water balance was evaluated for each time step (t – i.e. one month). The 4th-order Runge-Kutta integration method was employed (e.g. Zhang and Mitsch 2005) with flows being evaluated in the order they appear in the following equations:

$$SS_t = SS_{t-1} + P_t - E_t - OLF_t - TF_t - PER_t \quad (1)$$

Where:

P = precipitation which was evaluated as $P_t \times A$, where P_t is sub-catchment monthly precipitation and A is the sub-catchment area. P_t was derived from the CRU TS 3.0 dataset (Mitchell and Jones 2005) as the mean total monthly precipitation from the $0.5^\circ \times 0.5^\circ$ CRU grid cells falling within the respective sub-catchment. The number of cells contributing to catchment precipitation varied between eight (the sub-catchment draining to Tinkisso - a) and 27 (Douna - i) with a mean of 14.8. The area of each sub-catchment (A) was derived from the USGS GTOPO30 digital elevation model as described above;

E = sub-catchment evapotranspiration. Potential evapotranspiration for each sub-catchment was defined as $PET_t \times A$, where PET is the mean of the monthly Hargreaves total potential evapotranspiration (Hargreaves and Samani 1982) calculated for each of the $0.5^\circ \times 0.5^\circ$ CRU grid cells covering the respective sub-catchment. This PET method, which employs mean, minimum and maximum temperature from CRU TS 3.0 and extra-terrestrial solar radiation based on latitude, is often used in situations where data are insufficient to calculate Penman or Penman-Monteith (Allen *et al.* 1998, Thompson 2012). The actual evapotranspiration removed from a sub-catchment’s soil store was limited by the available storage (SS). Whilst actual evapotranspiration equalled or approached the volume of potential evapotranspiration during the wet season it was reduced as soil moisture was depleted through the dry season being limited to the volume available (i.e. $E_t = \min(SS_{t-1}, PET_t \times A)$). For example, through the complete simulation period (1950–2000) and across the 11 sub-catchments, actual evapotranspiration was on average 98.0% of potential volumes in the three wettest months (August–October). In most sub-catchments potential evapotranspiration demands were completely satisfied in at least September and up to four other wet season months. In contrast, at the height of the dry season (December–February) reduced soil storage resulted in actual evapotranspiration being equivalent to, on average, 11.9% of potential evapotranspiration;

OLF = overland flow evaluated as the difference between SS_{t-1} and a maximum soil store (Max_SS) which was determined through calibration. If $SS_{t-1} < Max_SS$, $OLF = 0$;

TF = throughflow evaluated as $SS_{t-1} \times RC_{TF}$ if $SS_{t-1} > Min_SS_{TF}$, where RC_{TF} is a reservoir constant with a possible value of between 0 and 1 and Min_SS_{TF} is a threshold soil store, both of which were determined through calibration. If $SS_{t-1} < Min_SS_{TF}$, $TF = 0$;

PER = percolation evaluated as $SS_{t-1} \times RC_{PER}$ if $SS_{t-1} > Min_SS_{PER}$, where RC_{PER} is a reservoir constant with a possible value of between 0 and 1 and Min_SS_{PER} is a threshold soil store, both of which were determined through calibration. If $SS_{t-1} < Min_SS_{PER}$, $PER = 0$;

$$GWS_t = GWS_{t-1} + PER_t - BF_t \quad (2)$$

Where:

BF = baseflow evaluated as $GWS_{t-1} \times RC_{BF}$ if $GWS_{t-1} > Min_GWS_{BF}$, where RC_{BF} is a reservoir constant with a possible value of between 0 and 1 and Min_GWS_{BF} is a threshold groundwater store, both of which were determined through calibration. If $GWS_{t-1} < Min_GWS_{TF}$, BF = 0;

$$CS_t = CS_{t-1} + OLF_t + TF_t + BF_t + UpQ_t - Q_t \quad (3)$$

Where:

UpQ = discharge from any upstream sub-catchment(s) simulated by respective sub-models;
 Q = river discharge from the sub-catchment evaluated as $CS_{t-1} \times RC_Q$, where RC_Q is a reservoir constant with a possible value of between 0 and 1 which was determined through calibration. Simulated monthly discharge volumes were distributed evenly throughout the month for comparison with observed mean monthly discharge.

The two largest dams above the Inner Niger Delta which were in operation for the modelled period or part thereof, the Sélingué Dam and the Markala Barrage, were included within the respective sub-models using results of previous analyses (Zwarts *et al.* 2005a). In the case of the Markala Barrage, simulated as being operational throughout the modelled period, withdrawals to the Office du Niger project were simulated as the mean monthly intakes to the scheme evaluated for the period 1988–2004. These withdrawals were removed from the simulated discharge of the Niger at Ke-Macina. The sub-model for the area draining to Sankarani included an element representing the Sélingué Dam that was defined as being in operation from 1982 (just before the end of the first quarter of the validation period). Simulated flows were retained within a store representing the reservoir behind the dam. Zwarts *et al.* (2005a) presented mean monthly inflows and outflows for the dam derived for the period 1982–2003. These were employed to define releases based on the percentages of the simulated annual inflow released in each month. In this way peak September discharges were, for example, reduced by 35.9% whilst, on average, dry season (December–May) discharges increased by 226.3%. The relatively simple approach represents the previously reported reductions in wet season peak flows and the increases in the dry season due to dam releases.

A final sub-model simulated the volume of water and, in turn, flood extent within the Inner Niger Delta. This was based on similar approaches adopted within models of the Delta and other large African floodplain wetlands (Sutcliffe and Parks 1987, 1989, Hollis and Thompson 1993a, Thompson and Hollis 1995). On a monthly basis the volume ($VIND$) of water stored within the Delta was evaluated as:

$$VIND_t = VIND_{t-1} + Q^{Ke-Macina}_t + Q^{Beney-Kegny}_t + PIND_t - EIND_t - IIND_t - Q^{Douna}_t \quad (4)$$

Where:

Q = the monthly volume of river discharge at the named gauging station. Inflows to the Delta from the Niger at Ke-Macina and the Bani at Beney-Kegny were provided by the discharges simulated by the hydrological model. Following the approach adopted by Hollis and Thompson (1993b) and Thompson and Hollis (1995) and using Global Runoff Data Centre (GRDC) gauging station records, a relationship was established between the mean monthly discharge at Douna downstream of the Delta and the weighted aggregate inflow (WAI_{inflow}) of the combined mean monthly discharges at Ke-Macina and Beney-Kegny (Inflow) during the four most recent months. The use of the four more recent months followed experiments similar to those undertaken by Thompson (1995) in which the number of months was varied between one and six in order to optimise the relationship between weighted aggregate inflow and discharge at Douna. The weights associated with each of the four months (which summed to 1.0) were varied to optimise the relationship shown in Figure 2a:

$$Q^{Douna}_t = 1.52 \times 10^9 \times \log(\text{WAInflow}_t) - 3.00 \times 10^{10} \quad (5)$$

Where:

$$\text{WAInflow} = (0.12 \times \text{Inflow}_t) + (0.18 \times \text{Inflow}_{t-1}) + (0.53 \times \text{Inflow}_{t-2}) + (0.17 \times \text{Inflow}_{t-3}) \quad (6)$$

Data availability limited this analysis to 1953–1992 whilst further periods of missing data for one or more stations of 1–6 months duration and in a few cases over a year (most notably 1981–1986 for which records for the inflows were not available) further impacted the data used in the analysis. Figure 2b demonstrates, for the period of available data, a close agreement between observed discharges at Douna and those derived using this approach;

PIND = precipitation over the Inner Niger Delta which was evaluated as $P_t \times \text{AIND}$ where P_t is the mean monthly precipitation for the CRU TS 3.0 grid cells covering the extent of the Delta and AIND is the extent of inundation evaluated using a synthetic volume/area relationship: $\text{AIND}_t = a(\text{VIND}_t)^b$ where a and b are coefficients optimised during calibration with final values of 1.095 and 0.981 being close to those employed in similar models of African floodplains (e.g. Sutcliffe and Parks 1989, Thompson and Hollis 1995);

EIND_t = monthly evapotranspiration from the Inner Niger Delta. Using the approach employed in each of the sub-catchment models, potential evapotranspiration was defined as $\text{PET}_t \times \text{AIND}$, where PET is the mean of the Hargreaves PET calculated for the each of the CRU TS 3.0 grid cells covering the Delta. Since AIND was calculated by the model and varied during the simulation, the potential volume of evapotranspiration from the Delta was relatively small during periods of low flood extent so that the volume of actual evapotranspiration for the calibrated model only differed from the potential in three months (February in 1973, 1978 and 1994) throughout the complete simulation period of 1950–2000. In these cases, EIND was limited to the volume of storage that was available;

IIND = infiltration beneath inundated areas. This was evaluated as $I \times \text{AIND}$ where I is the infiltration rate. The latter term was varied during calibration with the final value of 0.1 m month^{-1} being close to that of Thompson (1995) and Thompson and Hollis (1995) in their model of the floodplains of the Hadejia-Nguru Wetlands, northeast Nigeria. As for EIND, infiltration was potentially limited by the volume of water within the floodplain (VIND) but only differed from the potential rate in the same three months as EIND.

Model calibration and validation

Model simulations covered the period 1950–2000 and this was split in two for calibration and validation (1950–1975 and 1976–2000, respectively). Calibration of the sub-catchment hydrological models was undertaken in a downstream sequence beginning at the upper sub-catchments and progressing to those draining to Ke-Macina and Beney-Kegny. No calibration for discharge at Dire below the Inner Delta was undertaken as this was simulated using the relationship between discharge at this location and at Ke-Macina and Beney-Kegny (equations 5 and 6). The calibration parameters described above (reservoir constants for throughflow, percolation, baseflow and channel flow, and the threshold storage volumes for overland flow, throughflow, percolation and baseflow) were manually adjusted and simulated discharges compared to observed river discharge from the gauging station at the downstream end of each sub-catchment. These data were obtained from the GRDC and were characterized by extended periods of missing data at some gauging stations that were particularly associated with the validation period (discussed below). In order to provide additional model validation, observed and simulated discharges were also compared for the central 1961–1990 period that provides the baseline period for climate change scenarios (discussed below).

Sub-catchment hydrological model performance was assessed quantitatively using the Nash-Sutcliffe coefficient (NSE, Nash and Sutcliffe 1970), the Pearson correlation coefficient (r) and the bias (Dv; Henriksen *et al.* 2003). The scheme of Henriksen *et al.* (2008) was used to classify model

performance as indicated by values of NSE and Dv. Comparisons between observed and simulated river regimes provided additional assessments of model performance.

Calibration and validation of the sub-model simulating Inner Niger Delta flood extent was achieved through manual optimisation of the terms in the model's volume/area relationship and the infiltration rate. Results were compared to the estimates of peak annual inundation provided by Zwarts and Grigoras (2005). These were based on a relationship between water levels within the Delta and remote sensing-derived flood extent and were available for 1956–2000 (i.e. most of the calibration period and the complete validation and baseline periods).

Climate change scenarios

Revised meteorological inputs for a 30-year period, the same duration as the baseline period of 1961–1990 against which scenario results were compared, for a series of climate change scenarios were derived using the ClimGen pattern-scaling technique (Arnell and Osborn 2006). This spatial scenario generator assumes that the spatial pattern of change in meteorological parameters (based on the SRES A2 emissions scenario), expressed as a change per unit of global mean temperature, is constant for a given GCM. This allows patterns of climate change to be scaled up and down in magnitude so that specific thresholds of global climate change can be investigated (Todd *et al.*, 2011). In common with the QUEST-GSI catchment modelling studies, scenarios were generated for a 2 °C prescribed increase in global mean temperature, the hypothesised threshold for 'dangerous' climate change, for seven GCMs: CCCMA CGCM3.1, CSIRO Mk3.0, IPSL CM4, MPI ECHAM5, NCAR CCSM30, UKMO HadGEM1 and UKMO HadCM3 (Table 1, Todd *et al.* 2011). These are exemplars from the CMIP-3 database (Meehl *et al.* 2007) and provide different representations of global climate features.

For each scenario, monthly total precipitation and minimum, mean and maximum temperatures were derived from ClimGen for the CRU TS 3.0 0.5° × 0.5° grid. Subsequently monthly total Hargreaves PET was calculated for each grid cell using the temperature data. Using the same approach as for the baseline period, gridded monthly precipitation and PET totals were averaged for each of the 11 sub-catchments of the hydrological model and for the area over the Inner Niger Delta to provide scenario meteorological inputs.

The period 1961–1990 was used as a baseline for comparison with scenario results. Throughout both the baseline and each scenario the two existing dams that are included in the model (Sélingué Dam and Markala Barrage), were simulated as being operational using the approaches described above. For the Markala Barrage this represented no change from calibration and validation simulations. The Sélingué Dam was, however, assumed to be in operation from the start of the baseline period instead of from 1982. Scenario-baseline differences could therefore be attributed to climate change related modifications to precipitation and evapotranspiration alone.

RESULTS

Model calibration and validation

Figure 3 shows observed and simulated monthly discharges for seven gauging stations for the period 1950–2000 with the calibration, validation and baseline periods indicated. The stations include those immediately upstream (Ke-Macina and Beney-Kegny) and downstream (Douna) of the Inner Niger Delta although the former are characterised by relatively poor observed data availability for the validation period. The other four stations are representative of results for sub-catchments further upstream and have the most complete discharge records. Good agreement between observed and simulated discharges is demonstrated. This is particularly evident for the calibration period although some overestimation is apparent in the latter part of the validation period, especially for Douna and Dire (discussed below). The generally wetter conditions of the 1950s and 1960s are reproduced whilst reductions in flow in later decades, especially the droughts

of the early 1970s and mid-1980s, are evident. More recently some years in the late 1990s witnessed an increase in river flows that is demonstrated in both observed and simulated discharges.

Model performance for all 12 gauging stations is quantified for the calibration, baseline and validation periods in Table 2. This also shows for each period and station the number of years for which different amounts of data (from a complete 12 months to no observations) are available. Data availability is relatively poor for the validation period and in most cases gaps are more frequent in the second half of this period, in particular from the end of the 1980s.

For the calibration period, model performance according to the values of DV is classified as “excellent” for nine gauging stations and “very good” for the remaining three. The values of NSE are classified as “excellent” for all the stations apart from Kouroussa (“very good”). The classification scheme of Henriksen *et al.* (2008) was devised for comparisons at a daily time step and higher NSE values are to be expected when aggregating to monthly mean discharges (Thompson *et al.* 2014). Increasing the lower boundaries for the “excellent” and “very good” classes to 0.90 and 0.75, respectively still results in model performance for the calibration period being at least “very good” for all the stations (“excellent” for five). Figure 4 further confirms the good performance of the model for the calibration period by presenting observed and simulated mean monthly discharges (i.e. the river regimes). Simulated regimes are derived from results for months in which observed data are available with records being reasonably complete in most cases (the exception is Banankoro for which a complete record is only available for five years whilst data are absent for 17 years).

Assessment of model performance at some gauging stations for the validation period is impacted by poor data availability, especially in the later part of the period. For example, whilst a complete record for Tinkisso is available for the first three years, data are absent from January 1979 (22 years). Sankarani, Bougouni, Pankourou and Beney-Kegny are missing 17 complete years of records and Ke-Macina 16 years (Table 2). Performance is still classified as either “excellent” or “very good” (“fair” in the case of NSE for Ke-Macina), with mean monthly discharges being reasonably well produced (Figure 4). However, short observational records inevitably mean that confidence in these results is less than those of the calibration period. Performance at the other stations above the Delta for which longer (but still not complete) records are available is classified as “excellent” or “very good” according to NSE values. However, overestimation of seasonal peaks results in the values of DV being classed as “fair”. For some (Kouroussa, Banankoro, and Koulikoro) DV is within 2% of the higher class boundary whilst for Douna the magnitude of overestimation is larger. Figure 3 shows that overestimation of peaks is most noticeable towards the end of the validation period. Overestimated discharges above the Delta have implications for simulated discharges at Dire, with model performance being classified as “fair” according to DV, but excellent for NSE. Discharge overestimation for the validation period could be attributable to a number of factors including land cover change and consequent impacts on rainfall-runoff characteristics. Alternatively, it could be linked to data quality / availability which particularly impact the latter half of the validation period. These factors are discussed below.

Since the baseline period ends just before that for which data quality issues are suspected, overestimation of discharge does not occur and mean monthly discharges are well reproduced (Figure 4). Model performance according to the value of DV is “excellent” at nine stations and “very good” at three (Table 2). The values of NSE are classified as “excellent” for nine stations and “very good” for the remaining three. With the higher class boundaries, three stations still attain the “excellent” classification, with the remainder being classed as “very good”.

Figure 5a shows simulated monthly flood extent within the Inner Niger Delta for the complete simulation period as well as the annual peak flood extents estimated by Zwarts and Grigoras (2005) for 1956–2000. The calibration, validation and baseline periods are also indicated. The large seasonality and inter-annual variations in flood extent replicate those discussed for simulated river flow and are similar to those reported for other West African floodplains (e.g. Thompson and Hollis, 1995). Flood extents are generally highest in the 1950s and 1960s and decline from the 1970s. The impacts of the droughts of the early 1970s and early 1980s, in

particular 1984, are clearly evident in both the simulated flood extents and those estimated by Zwarts and Grigoras (2005). Peak inundation is relatively stable between the mid-1980s and mid-1990s, whilst the last part of the simulation period witnesses some increases in flood extent.

Figures 5b-d compare the model's annual maximum flood extents with those of Zwarts and Grigoras (2005) for the calibration, baseline and validation periods. They also provide the corresponding regression equations, Pearson correlation coefficients (r) and average percentage bias in simulated peak flood extents (Dv). Generally good performance is indicated for the calibration and baseline periods. Annual peak flooding is overestimated by, on average, just under 3.3% for the calibration period whilst for the baseline it is underestimated by only 1.3%. Approximately equal numbers of annual peaks are over- and underestimated (simulated > Zwarts and Grigoras (2005) in 55% and 45% of years during the calibration and baseline periods, respectively). In both cases r exceeds 0.85 and the slope of the regression (F-stats: 1.62×10^{-6} and 3.33×10^{-12} , respectively) is close to the 1:1 line.

For the validation period, similarly close agreement for peak flood extents is indicated by the values of r and Dv and again an almost equal number of flood extents are overestimated (56%) and underestimated. However, the slope of the regression (F-stat: 6.91×10^{-8}) is notably steeper. Figure 5a shows relatively large overestimation of annual peaks towards the end of the period during which river flows are overestimated. Other potential causes for differences between simulated flood extents and those provided by Zwarts and Grigoras (2005) based on water levels and remote sensing may be related to changes in the floodplain (see Discussion section).

Overall, given the good model performance for both river flow and flood extent, in particular for the calibration and baseline periods, the latter of which is employed for assessing the impacts of climate change, the model is considered an appropriate tool to assess GCM-related uncertainty upon hydrological conditions within the Inner Niger Delta and its catchment.

Scenario climate

Baseline annual precipitation and PET, as well as percentage changes from these totals, for each of the seven GCM climate change scenarios are shown for the 12 sub-catchments in Table 3. Figure 6 shows mean monthly precipitation and PET for the baseline and each scenario for four representative sub-catchments.

There are considerable inter-GCM variations in scenario precipitation, including differences in the direction of change. The largest inter-GCM differences in absolute and percentage terms for change in mean annual precipitation over any sub-catchment are 542 mm and 32.2%, respectively, both for Kouroussa (b) whilst the corresponding smallest differences are 114 mm (Delta - l) and 16.6% (Douna - i), respectively. On average the inter-GCM range of change across the 12 sub-catchments is 289 mm or 23.6%.

IPSL and MPI project declining annual precipitation in all sub-catchments although the magnitudes of the declines are considerably higher for IPSL (Table 3). This GCM shows a west-east reduction in the size of these declines. In most sub-catchments, mean monthly precipitation declines in every month (Figure 6). The largest reductions occur early in the wet season. Mean annual precipitation for MPI also tends to decline from west to east over the western half of the catchment after which the declines then increase in magnitude. The western part of the catchment (sub-catchments a-g) experiences modest (average: 6.2%) increases in mid-late wet season (July-October) precipitation although larger reductions in May-June (average: 24.4%) account for the overall declines in annual totals (Figure 6). The period of increased monthly precipitation shortens to the east and over the Delta is limited to September and October.

Both CSIRO and HadCM3 show that, with the exception of Tinkisso (a), westerly sub-catchments (CSIRO: b-e, HadCM3: b-g) experience relatively modest increases whilst annual precipitation for sub-catchments further east decreases (except Beney-Kegny - k for HadCM3). Seasonal patterns of change for these two GCMs are, however, different. For HadCM3, mean monthly precipitation in the south and west (sub-catchments a-g) generally increases between July

and February with the largest absolute, but still relatively small (5–7%), increases occurring in August and September for those in the west and September and October further east. For CSIRO, increases in monthly precipitation for westerly sub-catchments are concentrated earlier in the year (May–September with precipitation in the latter increasing for all sub-catchments, mean 12.9%). Further east, notable increases in monthly precipitation are limited to September.

CCCMA and HadGEM1 show declines in annual precipitation in the west, an easterly reduction in the magnitude of these declines and an eventual increase in the east. The gradient of the eastward decline in the size of these changes is steeper for HadGEM1 and increases occur for Douna (i), Ke-Macina (j) and sub-catchments beyond. Increased annual precipitation for CCCMA is limited to Beney-Kegnay (k) and the Delta (l). September precipitation increases in all sub-catchments for HadGEM1 with the largest changes (>20%) occurring in the south-centre of the catchment (sub-catchments e–g). Expansion of increased precipitation into July and August causes the eastward shift in the direction of change in annual precipitation. For CCCMA, modest increases in monthly precipitation for sub-catchments to the west and south of Koulikoro (h) are limited to November and December. Increases in August and September precipitation for the last four sub-catchments (and July for the Delta, mean 2.2%) cause the small increases in annual totals.

NCAR shows a more complex spatial pattern in the direction of change in annual precipitation. Most sub-catchments along the southern border of the Upper Niger display very small increases (Table 3). Sub-catchments that are further north (Tinkisso – a, Koulikoro – h) or extend further north from the southern border (Banankoro – c) show modest declines in annual precipitation. Further north and east, annual precipitation increases through sub-catchments i–l, with the 14.4% increase over the Delta (l) being the largest of all the GCMs for this part of the catchment. Seasonal changes in precipitation follow a consistent east–west trend. In the far west, precipitation declines between May and September and increases in the other dry season months so that absolute values remain small (Figure 6). The number of wet season months in which precipitation declines is reduced further east (e.g. Bougouni – f: four, Douna – i: two) and over the Delta (l) precipitation increases in every month apart from the already very dry January.

Inter-GCM differences in PET are small in comparison to precipitation. All GCMs project increases in annual PET for all sub-catchments (Table 3). The mean inter-GCM range of change in annual PET across the 12 sub-catchments is 86 mm / 4.4%, compared to the previously reported 289 mm / 23.6% for annual precipitation. The largest and smallest inter-GCM differences for any sub-catchment, 97 mm / 4.9% (both for Douna – i) and 77 mm (Tinkisso – a) / 4.1% (Banankoro – c), respectively, are also smaller than those for precipitation.

Seasonal distribution of PET for each scenario is similar to the baseline (Figure 6). In most cases PET increases in every month and where decreases do occur (HadGEM1, NCAR) they are limited to one or two months when PET is relatively low. There is some consistency in the relative order of magnitude of changes projected by different GCMs. In the west (sub-catchments a–f) the smallest increases in annual PET are projected by NCAR, whilst HadGEM1 is responsible for the smallest changes over the eastern sub-catchments. This pattern is reversed for the second smallest increases. The average change in PET for these two GCMs is 3.0% and 2.8%, respectively. At the other extreme, HadCM3 projects the largest mean change in annual PET (6.8%) and is responsible for the largest changes over sub-catchments east of Sankarani (e). MPI has the second largest mean change in annual PET (6.4%) and projects the largest changes over the remaining sub-catchments.

Scenario river flow

Table 4 provides mean baseline discharges for all 12 gauging stations and percentage changes for the seven climate change scenarios. Baseline Q5 and Q95 discharges (discharges equalled or exceeded for 5% and 95% of the time, respectively) and the corresponding scenario percentage changes are also shown. Impacts on the seasonal distribution of river flow are summarised in Figure 7, which shows baseline and scenario mean monthly discharges for each gauging station.

Inter-GCM differences in discharge are in general larger than those for precipitation and PET. For example, the largest inter-GCM range of change in mean discharge at any gauging station (Douna – i) is 79.2% (–57.0%–22.2%) whilst the smallest (Dire – l) is 42.8% (–42.5%–0.3%). The average range of change between the seven GCMs across the 12 gauging stations is 61.6%. The magnitude and spatial patterns of change in mean, peak and low discharges therefore vary considerably between the different GCMs.

The largest change in mean discharge of any sign for all 12 gauging stations is associated with IPSL, one of two GCMs projecting catchment-wide precipitation declines and with the largest reductions in annual precipitation. Mean discharge declines by over 50% at eight stations (Table 4) whilst the magnitude of the declines at all stations exceeds the absolute values of bias (D_v) reported for the calibrated model, even for the validation period during which discharges are overestimated (Table 2). Q5 discharges also decline across the catchment although the percentage reductions are 10–15% lower than those for mean flow. Conversely, percentage reductions in low flows (Q95 discharges) are larger. In the upper Bani (Bougouni – f, Pankourou – g, and Douna – i) very low baseline flows are eliminated completely. River flow declines throughout the year and in some cases (Tinkisso – a, Kouroussa – b, Koulikoro – h, Ke-Macina – i, Beney-Kegny – k), peak flows are delayed by one month compared to the baseline (October instead of September – Figure 7).

Smaller catchment-wide declines in annual precipitation for MPI, coupled with increases in some months, causes a different pattern in projected river flow. Eastern and western sub-catchments experience reductions in mean discharge with spatial variations reflecting those of precipitation (e.g. easterly reduction between Tinkisso – a and Kankan – d). The largest of these changes exceed the model bias (D_v) for the calibration and baseline period (and validation for Tinkisso – a). South-central sub-catchments, which experience the smallest declines in annual precipitation, show very small increases in mean discharge (comparable to absolute D_v values) due to higher late wet season precipitation. There is little change or, at some stations (e.g. Sankarani – e, Pankourou – g), small increases in peak flows (Figure 7, Q5 in Table 4). Declining precipitation at other times, coupled with higher PET, reduces low flows (no change at Bougouni – f).

CSIRO projects differences for the Niger and the Bani. In the far west of the former (Tinkisso – a, Kouroussa – b) mean discharge declines due to lower annual precipitation or modest precipitation gains coupled with larger increases in PET. Further west (Banankoro – c to Sankarani – e), larger increases in annual precipitation enhance mean discharge. Most of these changes are larger than the absolute values of D_v for the calibration, baseline and validation periods. Increased May–September precipitation increases peak flows (Q5, Table 4) and causes an earlier rise in the annual flood (e.g. Kankan – Figure 7). Low flows (Q95) increase (but remain very low) or show no change. Higher mean and peak flows in the upper Niger sustain similar increases further downstream (Koulikoro – h, Ke-Macina – j, although some changes are smaller than absolute values of D_v especially for the validation period) despite local precipitation declines and increased PET. Low flows do, however, decline. Declining precipitation over the Bani (sub-catchments f, g, i and k, Table 3) causes mean annual, Q5 and Q95 discharges to decline (no change in Q95 for Bougouni – f). The magnitude of these reductions generally increases in a downstream direction. Below the Delta (Dire – i) mean annual and Q5 discharges decline (baseline Q95 is $0 \text{ m}^3\text{s}^{-1}$) although by small amounts due to the enhanced flows in the Niger.

HadCM3 shows similar differentiation between the Niger and Bani in projected river flow changes. With the exception of Tinkisso (a), mean discharge increases at all gauging stations on the Niger above the Delta. However, due to the smaller precipitation increases over upstream sub-catchments combined with larger PET increases, discharge gains are smaller and very modest at downstream stations (less than absolute values of D_v at a number of stations) where declines in precipitation are projected (Table 4). The concentration of largest precipitation increases in the wettest months ensures that peak flows (Q5) increase. Some upstream increases in late wet season precipitation lead to increases in low flows (Q95) that are eliminated further downstream. Annual precipitation increases over upstream sub-catchments of the Bani (Bougouni – f, Pankourou – g; Table 3) do not offset elevated PET so that mean flows decline but by very small amounts. These

declines are enhanced at downstream stations (although differences are only greater than absolute Dv for the baseline period at Douna – i). Higher September precipitation results in very modest increases in Q5 for Bougouni (f) but not for Pankourou (g), whilst peak discharges decline further downstream. Low flows (Q95) show either no change (upstream) or decline (downstream). Beyond the Delta, projected discharge at Dire is barely distinguishable from CSIRO (Figure 7).

Similar results are obtained for CCCMA and NCAR although they project differences in scenario precipitation. Both simulate declines in mean, Q5 and Q95 discharges for all 12 gauging stations (no change in Q95 at Tinkisso – a, Table 4). For both scenarios the magnitude of changes in mean discharge exceed the absolute values of Dv for the calibration and baseline periods for all of the stations. This is repeated for CCCMA for the validation period whilst for NCAR changes exceed the absolute values of Dv for this period at all but two gauging stations). Discharge reductions are larger for CCCMA due to larger precipitation declines and larger PET increases. Although NCAR projects small precipitation increases for sub-catchments along the southern border of the Upper Niger, they are offset by slightly larger increases in PET so that discharges decline. For both GCMs the largest discharge reductions occur at stations on the Bani and its tributaries. For CCCMA, reductions in mean and Q5 discharges in sub-catchments f, g, i and k exceed 32% and 25%, respectively. With the exception of Tinkisso (a), reductions at other stations are below 25% and 21%, respectively. For NCAR, declines in mean discharge for Bani stations are all above (very close for Pankourou – g) 24% and most Q5 declines exceed 19%. Elsewhere declines do not exceed 18% and 16%, respectively.

Although HadGEM1 projects declines in mean annual precipitation over western sub-catchments (a–g), elevated September precipitation increases peak (Q5) discharges at all but two gauging stations (Table 4). Increases in September precipitation of over 20% coupled with the expansion of increases into July and August cause an increase in mean discharge at Sankarani (e), Bougouni (f) and Pankourou (g). The magnitudes of these changes are larger than the absolute values of Dv as the respective gauging stations for the calibration, baseline and validation periods. Increases are particularly large (>20%) for the last two stations due to large gains in peak flows (>30% in October, Figure 7). These changes, supplemented by locally higher precipitation, sustain increased mean discharge (> absolute DV for the three periods) further downstream on the Bani at Douna (i) and Beney-Kegny (k). High and low flows also increase. In contrast, increased mean discharge at Sankarani (e) and very modest precipitation increases in lower sub-catchments of the Niger do not offset declines from other Upper Niger tributaries. Mean discharge at Koulikoro (h) and Ke-Macina (j) therefore decline (although differences at both stations are only larger than absolute Dv for the baseline period). High flows do increase but by small and declining amounts whilst throughout the Niger (i.e. excluding the Bani) Q95 discharges decline. HadGEM1 is the only GCM to project increases, albeit very small, in mean and peak discharges below the Delta.

Scenario impacts on the Inner Niger Delta

The impacts of the seven GCM 2 °C climate change scenarios upon river inflow to the Inner Niger Delta are summarised in Figure 8. This provides the combined mean monthly inflows from the two gauging stations upstream of the wetland (Ke-Macina – j and Beney-Kegny – k) and percentage change from the baseline of the mean annual total inflows. Only one GCM, HadGEM1, projects an increase in annual inflows, albeit of only 3.9%. The higher inflows are due to the large projected increases in the discharge of the Bani under HadGEM1, although their impact is reduced by relatively small declines in discharge of the main Niger (Table 4) that contributes over three times more inflow than the Bani for the baseline. HadGEM1 inflows are higher than the baseline in every month apart from at the start of the annual flood (June–August) whilst peak (September and October) inflows increase by 4.0% and 16.4%, respectively. The larger increase for the second month causes a one-month shift in timing of mean annual peak inflows, although total discharge in October is only just above that in September.

The other six GCMs project declines in inflows although the magnitude of changes varies considerably. The smallest are associated with HadCM3 and CSIRO (−0.8% and −2.5%, respectively) both of which project small increases in inflows from the Niger that are offset by larger declines in the Bani. For HadCM3, increases are concentrated between October and January but are small, the largest being 3.3% for October. October inflows also increase for CSIRO but by only 0.8%, with the other increases being limited to June and July (83.3% and 23.5%, respectively although baseline inflows are low). The relatively small declines for the Niger and the Bani projected by MPI contribute to the very slightly larger (−3.9%) declines in annual inflows. Monthly increases (all <6%) are limited to the flood recession whilst peak inflows decline slightly (−3.1% and −0.3% for September and October, respectively).

The similar responses in river flow for NCAR and CSIRO lead to comparable seasonal distributions of river inflows to the Delta, with declines in annual totals of 18.1% and 26.1%, respectively. Mean inflows decline in every month with the peak months of September and October declining by 18.4% and 17.3%, respectively for NCAR and 22.8% and 22.4%, respectively for CSIRO. The substantial declines in river flow throughout the catchment for IPSL lead to a reduction in mean annual inflows of 52.7%, with declines occurring in every month. Inflows in September and October decline by 50.4% and 43.0%, the smaller reduction in the second month leading to a shift in the month of peak inflows, whilst the annual rise is delayed by the very large (79.2%) reduction in August discharges (Figure 8).

Figure 9 summarises the impact on the flood regime (mean monthly flood extent) of the Inner Delta for each GCM. In each case the baseline flood regime as well as the maximum and minimum monthly flood extents for both the baseline and scenario are shown. Given the ecological significance of peak floods for sustaining the Delta's fisheries, providing wildlife habitat (especially for waterbirds) and supporting human activities such as rice cultivation, Figure 10 summarises the impacts on the annual maximum flood extents. Figure 10a plots peak flood extents against the number of year in which they are equalled or exceeded for the baseline and each scenario. Changes from the baseline for the largest, mean and smallest annual peak flood extent within the 30 year simulation period are shown in Figure 10b–d, respectively. Changes in the mean annual maxima are close to those for November within the mean flood regime of Figure 9, with small differences attributable to differing annual peaks in some years.

Results for three scenarios show very limited impacts on flooding. The overall smallest changes are associated with HadCM3 that, as discussed, results in very small (0.8%) reductions in total river inflows. The mean flood regime, as well the maximum and minimum monthly flood extents, are barely discernable from those of the baseline (Figure 9). Similarly, the magnitude–frequency characteristics of annual peak flood extents are largely unaffected. The mean annual maximum declines by only 147 km² (1.0%) and the maximum by 44 km² (0.2%). The smallest annual peak does increase (221 km² or 6%) but this does not reflect a consistent trend for dry years (the next smallest annual peak declines). Overall, just over half of the points along the magnitude–frequency line for HadCM3 are below the baseline but differences in either direction are small.

The scenario flood regimes for CSIRO and MPI are very similar with only modest reductions in mean, maximum and minimum monthly mean flood extents (Figure 9). For MPI the three monthly mean flood extents decline in every month whilst for CSIRO very small increases for each occur in July and August. On average, the seasonal (November) peak of the mean regime declines by only 664 km² (4.8%) and 489 km² (3.5%), respectively. The smaller reduction for MPI despite the slightly larger decrease in annual river inflows (3.9% compared to 2.5% for CSIRO) is due to the smaller reduction in peak (September) inflows (Figure 8). The magnitude–frequency lines for the annual peak flood extents for both GCMs generally drop below the baseline. For CSIRO only two points (6.7% of the total, the 21st and 28th largest annual maxima) are above the baseline, whilst for MPI the corresponding number is six (20%). These are, with the exception of the greatest annual peak that declines, the larger annual maximum flood extents (Figure 10). The mean annual maximum declines by 679 km² (4.8%) and 518 km² (3.6%) for CSIRO and MPI, respectively.

CCCMA and NCAR result in larger reductions in flooding. In both cases the mean, maximum and minimum monthly mean flood extents decline in every month (Figure 9). Larger changes occur for CCCMA than for NCAR due to the greater declines in annual river inflows (CCCMA: -26.1% ; NCAR: -18.1%). The mean November peak declines by 4283 km^2 (31%) and 3018 km^2 (21.9%), respectively with comparable reductions in the peak maximum and minimum monthly means. These changes are reflected in the magnitude-frequency lines for annual peak flood extents (Figure 10a). Peak extents decline for all frequencies with the largest declines occurring for CCCMA. Changes in the mean annual maximum are comparable to those for November within the mean flood regime (CCCMA: $-4151 \text{ km}^2 / -29.1\%$; NCAR: $-2885 \text{ km}^2 / -20.2\%$; Figure 10c), whilst reductions in the largest annual maximum flood extents are similarly larger for CCCMA than NCAR (26.0% and 12.1% , respectively, Figure 10b). Differences between the two GCMs are reduced for smaller annual peak flood extents with, for example, the smallest annual peak declining by 34.8% and 34.2% respectively (Figure 10d).

As a result of inflows to the Delta more than halving for IPSL (-52.7%), this scenario simulates the largest reductions in flood extent. The mean, maximum and minimum flood regimes decline in all 12 months with the seasonal peak for the mean regime undergoing a reduction of 7903 km^2 (57.3% , Figure 9). Equivalent changes are indicated in the magnitude-frequency line for the annual maxima (Figure 10). Reductions for a given frequency range from 47.8% – 68.4% with the smaller, more frequent peak annual flood extents generally undergoing the largest reductions.

The only GCM leading to increases in flooding is HadGEM1, the one GCM that projects increased river inflow together with local increases in precipitation over the Delta (Table 3). However, in comparison to the declines projected for some GCMs, increases in flooding are relatively small. Flood extents for the mean, maximum and minimum flood regimes increase between October and June but decline slightly between July and September as a result of the moderately lower river inflows during this period (Figure 9). On average, the flood extent in November, which is still the peak month despite the delay in mean peak river inflows, increases by 1405 km^2 (10.2%). The delay in peak inflows is responsible for the subsequent increase in flooding throughout the recession period. The magnitude-frequency line for HadGEM1 shows a near consistent (28 out of 30 years) increase in flood extent for a given frequency (Figure 10a). The smallest changes are generally for the smallest peak flood extents ($+4.4\%$ for the smallest, Figure 10d; $+2.6\%$ the average for the smallest five) with the largest increases occurring for the larger extents ($+14.6\%$ for the largest, Figure 10b; $+13.3\%$ the average for the largest five).

DISCUSSION

Model performance for river flow for the 25-year long calibration and the 30-year long baseline periods is classified as either “excellent” or “very good”. It is at least as good, and in some cases superior, to other catchment models employed within the QUEST-GSI project to assess the impacts of the same climate change scenarios as those employed in the current study (e.g. Hughes *et al.* 2011, Kingston *et al.* 2011, Nóbrega *et al.*, 2011, Thorne, 2011). The model’s simulated annual flood peaks for these two periods also compare favourably with estimates of actual flood extents. Given these results, use of the model to simulate the impacts of climate change is justified with the second of these two periods providing the baseline against which scenarios results are compared. Whilst the model clearly simulates the seasonality and inter-annual variability in discharges for the more recent 25-year long validation period, discharges are overestimated, most obviously from the 1990s. Similarly, simulated flood extents are generally overestimated.

A possible explanation for the overestimation of discharge and flood extent could be changes in catchment characteristics. Elsewhere, land cover change due to removal of natural vegetation has been implicated in modified runoff coefficients (e.g. Lacombe *et al.* 2010) that may impact hydrological model performance (Thompson *et al.* 2013). Widespread declines in vegetation cover have been reported for the Sahelian region (e.g. Diello *et al.* 2005, Liéou *et al.* 2005, Leblanc *et al.* 2008). Such changes could not be included in the model given its empirically

established calibration parameters. Instead an alternative modelling approach permitting temporally varying land cover would be required. However, declines in Sahelian vegetation and consequent alterations to soil hydrodynamic properties have been shown to increase runoff (e.g. Descroix *et al.* 2009, Amogu *et al.* 2010), a phenomenon used to explain the “Sahelian Paradox” (Albergel 1987) whereby discharge has increased despite declining precipitation. It would therefore be expected that the model would underestimate instead of overestimating discharges and flood extent.

Issues associated with the data employed within the model might mask impacts of changing catchment runoff characteristics. Declining hydrometeorological data quantity and quality is an acknowledged problem throughout much of Sub-Saharan Africa (e.g. World Bank *et al.* 1993, Farquharson 2007). In the current study, reductions in the availability of discharge data for a number of gauging stations, especially in more recent decades, impact the appraisal of model performance during the validation period. It also prevents a definitive assessment of whether overestimation of discharge is a catchment-wide issue. Similarly, empirical methods employed in the model, such as the approach used to define outflows from the Inner Niger Delta from simulated inflows, were based on restricted time periods due to data availability. In particular, observed discharge for the two inflow gauging stations was unavailable beyond 1992. This prevents the inclusion of any temporal changes in such relationships which in this case might result from natural channel evolution including the influence of aquatic vegetation (e.g. Goes 2002) as well as human activities such as dykes and sluices associated with rice cultivation (Zwarts and Kone 2005b). Such changes would also impact the relationship between volume and flood extent used within the model that is assumed to be constant. They would also alter the relationship between water level and inundation that was used by Zwarts and Grigoras (2005) to derive the annual maximum flood extent time series. This relationship was based on satellite imagery from 1985–2003, a period when flood extents were in most cases lower than those experienced in the 1950s and 1960s.

The potential for changes identified in West African rainfall to be artefacts of changing meteorological station numbers and locations has been reported (e.g. Chappell and Agnew 2004). The decline in the region’s hydrometeorological monitoring networks may have impacted the gridded meteorological data used to force the hydrological model. Gridded datasets, such as CRU, are widely employed in catchment modelling with, for example, many of the models used in the QUEST-GSI project using CRU meteorological inputs (e.g. Nóbrega *et al.* 2011, Thorne 2011, Xu *et al.* 2011). These datasets are easily accessed and readily sampled for areas of interest. They are particularly valuable where station records may be difficult to acquire. However, they clearly rely on data provided by observation networks. At the start of the modelling period used in the current study ten stations within the basin and a further 58 within 200 km of its boundary are listed as contributing to CRU TS 3.0. These stations are distributed relatively evenly through and around the basin. By the mid-1960s, the number of stations increases and then remains stable at between 15–16 and 95–100, respectively until the beginning of the 1990s. Thereafter a precipitous decline in the number of stations begins so that by 2000 only 6 and 14, respectively remain. Up to 22 stations within the larger area cease to provide data in any one year. The loss of many stations in the relatively dry northeast is particularly noticeable. Such declines in the number of meteorological stations, which Harris *et al.* (2014) demonstrate is repeated throughout Africa, have implications for the degree to which catchment meteorological conditions are represented. Similar issues affecting gridded precipitation datasets may have impacted calibration of hydrological models of other parts of the world (e.g. Hughes *et al.* 2011, Kingston *et al.* 2011, Thompson *et al.* 2014a). The current study demonstrates that when using gridded datasets within hydrological models, especially for extended simulation periods over which changes in observation networks are more likely, it is important to review the stations contributing to the datasets as a potential source of additional uncertainty. Diagnostics for the most recent CRU TS3.10 dataset include the number of stations used in the interpolation process for a given cell enabling objective assessment of the reliability of the dataset (Harris *et al.* 2014).

Uncertainty in scenario meteorological inputs to the hydrological model is dominated by projected change in precipitation. Of the 84 sub-catchment / GCM combinations (12 sub-

catchments, seven GCMs) declines in mean annual precipitation are projected for 57 (just under 68%). Whilst some GCMs show catchment-wide or near catchment-wide reductions in precipitation (CCCMA, IPSL, MPI) others show spatially varying directions of change. Seasonal changes in precipitation also vary between GCMs. In contrast, all GCMs project higher annual PET totals and, in most cases, PET is higher throughout the year. Inter-GCM uncertainty in the projected changes in PET is considerably smaller than precipitation. For example, the mean absolute inter-GCM range of change in annual precipitation across the 12 sub-catchments (289 mm) is over three times that of PET (86 mm). Differences for the mean percentage range of change are larger still with that of precipitation (23.6%) exceeding PET (4.4%) by nearly 5.5 times.

The dominance of precipitation in the inter-GCM uncertainty of projected meteorological conditions reflects earlier results using the same scenarios (Kingston and Taylor 2010, Kingston *et al.* 2011, Singh *et al.* 2011; Thompson *et al.* 2013) although inter-GCM differences in the direction and relative magnitude of precipitation changes varied between these studies. There is some consistency in the relative magnitude of PET changes between the different GCMs for the current study and earlier investigations. In accordance with the results presented herein, Singh *et al.* (2011) and Thompson *et al.* (2013) both identified HadCM3 as providing some of the largest annual increases despite the very different locations of their catchments (northeast India and the southeast Asia). Similarly, in common to the Upper Niger, both of these earlier studies showed that some of the smallest changes were associated with NCAR, the GCM that also provided the smallest changes in temperature over Uganda (Kingston and Taylor 2010).

The inter-GCM ranges of change in discharge are larger than those for both precipitation and PET (average range of change in mean discharge across the 12 gauging stations: 61.6%). Of the 84 gauging stations / GCM combinations, 64 (just over 76%) experience declines in mean discharge. This is a larger proportion than for declines in precipitation since in some cases elevated PET offsets relatively small gains in precipitation. However, there is not a perfect match between declining sub-catchment precipitation and reductions in discharge. In some cases (e.g. HadGEM1) large increases in peak wet season precipitation, despite overall declines in annual totals, increase wet season discharges, as reflected in the smaller number of gauging stations (55 or 67%) for which Q5 discharges decline. It is possible for these enhanced wet season flows to produce an overall increase in mean annual discharge. In other cases (e.g. CSIRO), relatively large increases in precipitation over upstream sub-catchments lead to increases in discharge that persist further downstream where local declines in precipitation and increases in PET are projected. Thompson *et al.* (2014a) demonstrated similar patterns for the Mekong highlighting the potential for alternative PET methods, which exhibited different magnitudes of change for the same scenario, to influence the point along the river system at which increases in discharge switch to decreases. Assessment of this additional source of uncertainty for the Upper Niger could be investigated through the recalibration of the model using PET calculated using a number of different methods.

Only one GCM (HadGEM1) projects increases in the mean annual inflows to the Inner Niger Delta. These modest (3.9%) increases lead to a mean gain compared to the baseline of 1405 km² (10.2%) in peak flood extent within this internationally important wetland and subsequently more extensive inundation during the recession period. Mean annual inflows to the Delta decline for the remaining six GCMs although in three cases, these reductions are less than 5%. As a result, flooding is only marginally reduced from the baseline. In contrast, reductions in the range of 18.1%–52.7% for the three remaining GCMs have a progressively larger impact on flooding. Although seasonality in the flood cycle remains the same, the annual peak flood extent declines by between 3018 km² (21.9%) and 7903 km² (57.3%).

Differences in projected changes in river flow and flood extent for the seven GCMs point to considerable uncertainty in the environmental and water resource implications of climate change. Implications will vary between GCMs as well as within different parts of the catchment, at least for those scenarios with spatially varying changes in river flow. The regimes of a river and its floodplains, which can be characterised by the variability, magnitude, frequency, duration, timing and rate of change of flow and flooding, is central to sustaining biodiversity and ecosystem integrity

(e.g. Poff *et al.* 1997). They in turn underpin ecosystem services. Increased discharge may, for example, benefit fish populations by facilitating migration onto more extensive floodplain nursery areas (Welcomme 1986, Nestler *et al.* 2012) with obvious benefits for those people who depend on fisheries. Enhanced river flow and flooding could sustain aquatic habitats and provide opportunities for water-related human activities such as agriculture. Conversely, as witnessed in many African river systems (e.g. Drijver and Marchand 1985, Adams 1992), lower river flows and flood extents may lead to declines in floodplain habitats and the wildlife that depend upon them as well as reductions in the opportunities for people. Changing flood patterns within the Inner Niger Delta have already impacted agricultural activities, especially rice cultivation, fishing and grazing (Goosen and Kone 2005, Zwarts and Diallo 2005, Zwarts and Kone 2005b).

Determining the precise nature of such impacts is not a trivial undertaking. Environmental flow methodologies, such as the widely used Range of Variability Approach that employs Indicators of Hydrological Alteration (IHA), provide statistical techniques for comparing natural and altered flow regimes (Richter *et al.* 1996, 1997). Thompson *et al.* (2014b), for example, employed a modified IHA approach (Laizé *et al.* 2014) to investigate changes in environmental flows throughout the Mekong. This included the development of a risk-based assessment of the magnitude of change. Adoption of such an approach, with potential modifications to include simulated flood extent, could provide an initial means of addressing uncertainty in the ecological impacts of projected hydrological change.

GCM-related uncertainty for future hydrometeorological conditions for the Upper Niger including flooding within the Delta could be constrained through the development of GCM reliability ratings by comparing simulated and observed climate (e.g. Perkins *et al.* 2007, Maxino *et al.* 2008, Ghosh and Mujumdar 2009). Such an evaluation of GCM performance is, however, beyond the scope of the current study. Additionally, the climate change scenarios employed herein use the previous generation of GCMs. The more recent Coupled Model Intercomparison Project phase 5 (CMIP5) provides results from a larger ensemble of 41 GCMs (Knutti and Sedlacek 2013). Further investigation of GCM-related uncertainty on meteorological conditions and, using the hydrological model, river flow and flood extent within the Upper Niger using the CMIP5 results would be a valuable extension of the current study. Such an assessment could be undertaken using the methodology developed by Ho *et al.* (2015).

Beyond the impacts of climate change, additional uncertainty over future river flows within the Upper Niger and flood extent within the Inner Delta is associated with water resource management, in particular dams. Across Africa, and elsewhere, dams have had major impacts on river flow and inundation of floodplain wetlands (e.g. Lemly *et al.* 2000, Mumba and Thompson 2005, Kingsford *et al.* 2006). The model does include the impacts of the two existing schemes that impact river flow and which were operational throughout or during part of the model period. Changes in the operation of these dams in the face of climate change are, however, a potential source of uncertainty. The impacts of the Talo Dam on the Bani, constructed after the end of the modelled period, are not included and given available information are uncertain. The possible construction of the Formi hydropower dam which will also support an irrigated area of 30 000 ha, will impact flows on the Niandan tributary and in turn the Niger. The precise impacts of the dam are also uncertain although Zwarts and Grigoras (2005) argue that the changes in wet and dry season flows are likely to be comparable to those due to the Sélingué Dam but of larger magnitude since it has a storage capacity almost three times as large. Diversion of water to such a large irrigated area will inevitably reduce total river flows. The potential impacts of another reservoir, Djenné, on the Bani are currently even more difficult to assess due to limited information on its design and operation (Zwarts *et al.* 2005a). As Van Dijk *et al.* (2008) suggest, additional unforeseen modifications to water management in response to climate-change, which may in turn be driven by social, economic and policy changes, represent another important, but difficult to assess, source of uncertainty.

CONCLUSIONS

A semi-distributed, conceptual hydrological model of the Upper Niger, which includes an element simulating flood extent within the Inner Niger Delta, successfully simulates discharge at 12 gauging stations and annual peak flood extent for the second half of the 20th Century. Performance for much of the period is classed as “excellent” or “very good”. Overestimation of discharge and flood extent for the last decade of the simulation period may be associated with changing land cover or, perhaps more likely, declines in hydrometeorological monitoring networks. These limit robust assessments of model performance for the last part of the simulation period.

Scenarios for a 2 °C prescribed increase in global mean temperature, the hypothesised threshold for ‘dangerous’ climate change, for seven GCMs, demonstrate that inter-GCM uncertainty is far greater for precipitation than PET. The inter-GCM range of change in mean annual precipitation is three to five times as large as that of PET. Whilst PET increases in all sub-catchments for all the scenarios, precipitation both increases and decreases, with some GCMs projecting spatial variations in the direction of change. Declines in precipitation are dominant, occurring in 68% of the 84 sub-catchment / GCM combinations.

Projected discharges are also dominated by declines (mean flow is lower in 76% of the 84 gauging station / GCM combinations). Only one GCM (HadGEM1) simulates increases (of only 3.9%) in annual river inflow to the Inner Niger Delta. Simulated flood extents increase as a result (mean peak +10.2%). The remaining GCMs project widely varying reductions in annual inflow of between 0.8% and 52.7%. Minor reductions in flood extent are simulated for three GCMs that project declines in inflow of less than 5%. However, larger inflow reductions of between 18.1% and 52.7% for other GCMs induce substantial modifications to flooding with in the extreme case (IPSL) the mean peak flood extent declining by 57.3%.

Possible extension of this research could include the application of environmental flow approaches to assess the risks of ecological change due to modified river flows and flooding. These changes could be used to infer the impacts on ecosystem services provided by the river and its floodplains. Expansion of the investigation of inter-GCM related uncertainty through the use of more recent and a larger number of GCMs, such as those from the Coupled Model Intercomparison Project phase 5, could also be a valuable next step.

Acknowledgements: ClimGen climate scenarios were generated by Tim Osborn at the Climatic Research Unit of the University of East Anglia. Valuable comments on a draft of the paper were provided by A.J. Green. Two anonymous reviewers provided additional comments that greatly improved the paper.

Funding: The present study develops earlier research supported by a grant from the UK Natural and Environmental Research Council under the Quantifying and Understanding the Earth System (QUEST) programme (Ref. NE/E001890/1).

References

Acreman, M.C., Blake, J.R., Booker, D.J., Harding, R.J., Reynard, N., Mountford, J.O. and Stratford, C.J., 2009. A simple framework for evaluating regional wetland ecohydrological response to climate change with case studies from Great Britain. *Ecohydrology*, 2, 1–17.

Adams, W.M., 1992. *Wasting the rain: rivers, people and planning in Africa*. London: Earthscan.

Albergel, J., 1987. Sécheresse, désertification et ressources en eau de surface: application aux petits bassins du Burkina Faso. In: S.I. Solomon, M. Beran and W. Hogg, eds. *The influence of climate change and climatic variability on the hydrologic regime and water resources*. Wallingford: IAHS, 355–365.

Allen, R.G., Pereira, L.S., Raes, D. and Smith, M., 1998. *Crop evapotranspiration – guidelines for computing crop water requirements*, FAO Irrigation and Drainage Paper 56. Rome: FAO.

Amogu, O., Descroix, L., Yéro, K.S., Le Breton E., Mamadou, I., Ali, A., Vischel, T., Bader, J-C., Moussa, I.B., Gautier, E., Boubkraoui, S. and Belleudy, P., 2010. Increasing river flows in the Sahel? *Water*, 2, 170–199.

Arnell, N.W. and Gosling, S.N., 2013. The impacts of climate change on river flow regimes at the global scale. *Journal of Hydrology*, 486, 351–364.

Arnell, N.W. and Osborn, T., 2006. *Interfacing climate and impacts models in integrated assessment modelling*, Tyndall Centre for Climate Change Research Technical Report 52. Southampton and Norwich: Tyndall Centre for Climate Change Research.

Baker, C., Thompson, J.R. and Simpson, M., 2009. Hydrological dynamics I: Surface waters, flood and sediment dynamics. In: E.B. Maltby and T. Barker, eds. *The wetlands handbook*. Chichester: Wiley-Blackwells, 120–168.

Bates, B.C., Kundzewicz, Z.W., Wu, S. and Palutikof, J.P., eds. 2008. *Climate change and water*, Technical paper of the Intergovernmental Panel on Climate Change. Geneva: IPCC Secretariat.

Beadle, L.C., 1974. *The inland waters of tropical Africa: an introduction to tropical limnology*. London: Longman.

Chappell, A. and Agnew, C.T., 2004. Modelling climate change in West African Sahel rainfall (1931–90) as an artifact of changing station locations. *International Journal of Climatology*, 24, 547–554.

Chiew, F.H.S., Vaze, J., Viney, N.R., Jordan, P.W., Perraud, J-M., Zhang, L., Teng, J., Young, W.J., Penaarancia, J., Morden, R.A., Freebairn, A., Austin, J., Hill, P.I., Wiesenfeld, C.R. and Murphy, R. 2008. *Rainfall-runoff modelling across the Murray-Darling Basin*. A report to the Australian Government from the CSIRO Murray-Darling Basin Sustainable Yields Project. Canberra: CSIRO.

Descroix, L., Mahé, G., Lebel, T., Favreau, G., Galle, S., Gautier, E., Olivry, J.C., Albergel, J., Amogu, O., Cappelaere, B., Dessouassi, R., Diedhiou, A., Le Breton, E., Mamadou, I. and Sighomnou, D., 2009. Spatio-temporal variability of hydrological regimes around the boundaries between Sahelian and Sudanian areas of West Africa: a synthesis. *Journal of Hydrology*, 90–102.

Drijver, C.A. and Marchand, M., 1985. *Taming the floods: environmental aspects of floodplain development in Africa*. Leiden: Centre for Environmental Studies, University of Leiden.

Diello, P., Mahé, G., Paturel, J.E., Dezetter, A., Delclaux, F., Servat, E. and Ouattara, F., 2005. Relationship between rainfall and vegetation indexes in Burkina Faso: a case study of the Nakambé Basin. *Hydrological Sciences Journal*, 50, 207–221.

Erwin, K.L., 2009. Wetlands and global climate change: the role of wetland restoration in a changing world. *Wetlands Ecology and Management*, 17, 71–84.

Farquharson, F., 2007. The deterioration in hydrometric data collection in Africa; what can be done about it? *Earth: Our Changing Planet. Proceedings of the International Union of Geodesy and Geophysics XXIV General Assembly*, 2–13 July 2007, Perugia, Italy.

Ghosh, S. and Mujumdar, P.P., 2009. Climate change impact assessment: uncertainty modelling with imprecise probability. *Journal of Geophysical Research*, 114, D18113.

Goes, B.J.M., 2002. Effects of river regulation on aquatic macrophyte growth and floods in the Hadejia-Nguru Wetlands and flow in the Yobe River, northern Nigeria; implications for future water management. *River Research and Applications*, 18, 81–95.

Goosen, H. and Kone, B., 2005. Livestock in the Inner Niger Delta. In: L. Zwarts, P. van Beukering, B. Kone and E. Wymenga, eds. *The Niger, a lifeline: effective water management in the Upper Niger Basin*. Lelystad: RIZA / Sévaré: Wetlands International / Amsterdam: Institute for Environmental Studies / Veenwouden: A&W Ecological Consultants, 121–135.

Gosling, S.N. and Arnell, N.W., 2011. Simulating current global river runoff with a global hydrological model: model revisions, validation and sensitivity analysis. *Hydrological Processes*, 25, 1129–1145.

Gosling, S.N., Taylor, R.G., Arnell, N.W. and Todd, M.C., 2011. A comparative analysis of projected impacts of climate change on river runoff from global and catchment-scale hydrological models. *Hydrology and Earth System Sciences*, 15, 279–294.

Graham, L.P., Andréasson J. and Carlsson, B., 2007. Assessing climate change impacts on hydrology from an ensemble of regional climate models, model scales and linking methods – a case study on the Lule River basin. *Climatic Change*, 81, 293–307.

Grove, A.T. ed. 1985. *The Niger and its neighbours: environmental history and hydrobiology, human use and health hazards of the major West African rivers*. Rotterdam: Balkema.

Haddeland, I., Clark, C., Franssen, W., Ludwig, F., Voß, F., Bertrand, N., Folwell, S., Gerten, D., Gomes, S., Gosling, S.N., Hagemann, S., Hanasaki, N., Heinke, J., Kabat, P., Koirala, S., Polcher, J., Stacke, T., Viterbo, P., Weedon, G. and Yeh, P., 2011. Multi-model estimate of the global water balance: setup and first results. *Journal of Hydrometeorology*, 12, 869–884.

Henriksen, H.J., Troldborg, L., Højberg, A.J. and Refsgaard, J.C., 2008. Assessment of exploitable groundwater resources of Denmark by use of ensemble resource indicators and a numerical groundwater–surface water model. *Journal of Hydrology*, 348, 224–240.

Henriksen, H.J., Troldborg, L., Nyegaard, P., Sonnenborg, T.O., Refsgaard, J.C. and Madsen, B., 2003. Methodology for construction, calibration and validation of a national hydrological model for Denmark. *Journal of Hydrology*, 280, 52–71.

Hollis, G.E. and Thompson, J.R., 1993a. Hydrological model of the floodplain. In: G.E. Hollis, W.M. Adams and M. Aminu-Kano, eds. *The Hadejia Nguru Wetlands: environment, economy and sustainable development of a Sahelian floodplain wetland*. Gland and Cambridge: IUCN, 69–80.

Hollis, G.E. and Thompson, J.R., 1993b. Water resource developments and their hydrological impacts. In: G.E. Hollis, W.M. Adams and M. Aminu-Kano, eds. *The Hadejia Nguru Wetlands: environment, economy and sustainable development of a Sahelian floodplain wetland*. Gland and Cambridge: IUCN, 149–190.

Hargreaves, G.H. and Samani, Z.A., 1982. Estimating potential evapotranspiration. *Journal of the Irrigation and Drainage Division, American Society of Civil Engineers*, 108, 225–230.

Harris, I., Jones, P.D., Osborn, T.J. and Lister, D.H., 2014. Updated high-resolution grids of monthly climatic observations – the CRU TS3.10 Dataset. *International Journal of Climatology*, 34, 623–642.

Ho, J.T., Thompson, J.R. and Brierley, C. 2015. Projections of hydrology in the Tocantins-Araguaia Basin, Brazil: uncertainty assessment using the CMIP5 ensemble. *Hydrological Sciences Journal*. Author Manuscript Online (DOI 10.1080/02626667.2015.1057513)

Hughes, D.A., Kingston, D.G. and Todd, M.C., 2011. Uncertainty in water resources availability in the Okavango River basin as a result of climate change. *Hydrology and Earth System Science*, 15, 931–941.

John, D.M., Lévêque, C. and Newton, L.E., 1993. Western Africa. In: D.F. Whigham, D. Dykyjová and S. Hejný, eds. *Wetlands of the World: inventory, ecology and management. Volume 1*. Dordrecht: Kluwer, 47–78.

Kingsford, R.T., Lemly, A.D. and Thompson, J.R., 2006. Impacts of dams, river management and diversions on desert rivers. In: R.T. Kingsford, ed. *Ecology of desert rivers*. Cambridge University Press: Cambridge, 203–247.

Kingston, D.G. and Taylor, R.G., 2010. Sources of uncertainty in climate change impacts on river discharge and groundwater in a headwater catchment of the Upper Nile Basin, Uganda. *Hydrology and Earth System Science*, 14, 1297–1308.

Kingston, D.G., Thompson, J.R. and Kite, G., 2011. Uncertainty in climate change projections of discharge for the Mekong River Basin. *Hydrology and Earth System Science*, 15, 1459–1471.

Knutti, R. and Sedlacek, J., 2013. Robustness and uncertainties in the new CMIP5 climate model projections. *Nature Climate Change*, 3, 369–373.

Kundzewicz, Z.W., Mata, L.J., Arnell, N.W., Döll, P., Kabat, P., Jiménez, B., Miller, K.A., Oki, T., Sen, Z. and Shiklomanov, I.A., 2007. Freshwater resources and their management. In: M.L. Parry, O.F. Canziani, J.P. Palutikof, P.J. van der Linden and C.E. Hanson, eds. *Climate change 2007: impacts, adaptation and vulnerability*. Contribution of Working Group II to the Fourth Assessment Report of the Intergovernmental Panel on Climate Change. Cambridge: Cambridge University Press, 173–210.

Laizé, C.L.R., Acreman, M., Schneider, C., Dunbar, M.J., Houghton-Carr, H.A., Flörke, M. and Hannah, D.M., 2014. Projected flow alteration and ecological risk for pan-European rivers. *River Research and Applications*, 30, 299–314.

Leblanc, M., Favreau, G., Massuel, S., Tweed, S., Loireau, M. and Cappelaere, B., 2008. Land clearance and hydrological change in the Sahel: SW Niger. *Global Planetary Change*, 61, 49–62.

Lacombe, G., Pierret, A., Hoanh, C.T., Sengtaeuanghoung, O., and Noble, A.D., 2010. Conflict, migration and land-cover changes in Indochina: A hydrological assessment. *Ecohydrology*, 3, 382–391.

Lemly, A.D., Kingsford, R.T. and Thompson, J.R., 2000. Irrigated agriculture and wildlife conservation: conflict on a global scale. *Environmental Management*, 25, 485–512.

Liéno, G., Mahé, G., Olivry, J.C., Naah, E., Servat, E., Sigha-Nkamdkou, L., Sighomnou, D., Ngoupayou, J.N., Ekodeck, G.E. and Paturel, J.E. 2005. Regimes of suspended sediment flux in Cameroon: review and synthesis for the main ecosystems; climatic diversity and anthropogenic activities. *Hydrological Sciences Journal*, 50, 111–123.

Maxino, C.C., McAvaney, B.J., Pitman, A.J. and Perkins, S.E., 2007. Ranking the AR4 climate models over the Murray-Darling Basin using simulated maximum temperature, minimum temperature and precipitation. *International Journal of Climatology*, 28, 1097–1112.

Meehl, G.A., Covey, C., Delworth, T., Latif, M., McAvaney, B., Mitchell, J.F.B., Stouffer, R.J. and Taylor, K.E., 2007. The WCRP CMIP3 Multimodel Dataset: A new era in climate change research. *Bulletin of the American Meteorological Society*, 88, 1383–1394.

Mitchell, T.D. and Jones, P.D., 2005. An improved method of constructing a database of monthly climate observations and associated high-resolution grids. *International Journal of Climatology*, 25, 693–712.

Mumba, M. and Thompson, J.R., 2005. Hydrological and ecological impacts of dams on the Kafue Flats floodplain system, southern Zambia. *Physics and Chemistry of the Earth*, 30, 442–447.

Nestler, J.M., Pompeu, P.S., Goodwin, R.A., Smith D.L., Silva L.G.M, Baigun, C.R.M. and Oldani, N.O., 2012. The River Machine: A template for fish movement and habitat, fluvial geomorphology, fluid dynamics and biogeochemical cycling. *River Research and Applications*, 28, 490–503.

Nóbrega, M.T., Collischonn, W., Tucci, C.E.M. and Paz, A.R., 2011. Uncertainty in climate change impacts on water resources in the Rio Grande Basin, Brazil. *Hydrological Sciences Journal*, 15, 585–595.

Perkins, S.E., Pitman, A.J., Holbrook, N.J. and McAvaney, B.J., 2007. Evaluation of the AR4 climate models' simulated daily maximum temperature, minimum temperature and precipitation over Australia using probability density functions. *Journal of Climate*, 20, 4356–4376.

Poff, N.L., Allan, J.D., Bain, M.B., Karr, J.R., Prestegard, K.L., Richter, B., Sparks, R. and Stromberg, J., 1997. The Natural Flow Regime: a new paradigm for riverine conservation and restoration. *BioScience*, 47, 769–784.

Prudhomme, C. and Davies, H., 2009. Assessing uncertainties in climate change impact analyses on the river flow regimes in the UK. Part 1: baseline climate. *Climatic Change*, 93, 177–195.

Ramsar Bureau. 2002. *Climate Change and Wetlands: Impacts, Adaptations and Mitigation*. Ramsar COP8 DOC.11. Gland: Ramsar Convention Bureau.

Richter, B.D., Baumgartner, J.V., Powell, J. and Braun, D.P., 1996. A method for assessing hydrologic alteration within ecosystems. *Conservation Biology*, 10, 1163–1174.

Richter, B.D., Baumgartner, J.V., Wigington, R. and Braun, D.P., 1997. How much water does a river need? *Freshwater Biology*, 37, 231–249.

Singh, C.R., Thompson, J.R., French, J.R., Kingston, D.G. and Mackay, A.W., 2010. Modelling the impact of prescribed global warming on runoff from headwater catchments of the Irrawaddy River and their implications for the water level regime of Loktak Lake, northeast India. *Hydrology and Earth System Science*, 14, 1745–1765.

Singh, C.R., Thompson, J.R., Kingston, D.G. and French, J.R., 2011. Modelling water-level options for ecosystem services and assessment of climate change: Loktak Lake, northeast India. *Hydrological Sciences Journal*, 56, 1518–1542.

Sutcliffe, J.V. and Parks, Y.P., 1987. Hydrological Modelling of the Sudd and Jonglei Canal. *Hydrological Sciences Journal*, 32, 143–159.

Sutcliffe, J.V. and Parks, Y.P., 1989. Comparative water balances of selected African wetlands. *Hydrological Sciences Journal*, 34, 49–62.

Thompson, J.R. 1995. *Hydrology, water management and wetlands of the Hadejia Jama'are Basin, Northern Nigeria*. PhD Thesis, University of London.

Thompson, J.R., 1996. Africa's floodplains: a hydrological overview. In: M.C. Acreman and G.E. Hollis, eds. *Water management and wetlands in Sub-Saharan Africa*. Gland: IUCN, 5–20.

Thompson, J.R., 2012. Modelling the impacts of climate change on upland catchments in southwest Scotland using MIKE SHE and the UKCP09 probabilistic projections. *Hydrology Research*, 43, 507–530.

Thompson, J.R., Gavin, H., Refsgaard, A., Refstrup Sørensen, H. and Gowing, D.J., 2009. Modelling the hydrological impacts of climate change on UK lowland wet grassland. *Wetlands Ecology and Management*, 17, 503–523.

Thompson, J.R., Green, A.J., Kingston, D.G. and Gosling, S.N., 2013. Assessment of uncertainty in river flow projections for the Mekong River using multiple GCMs and hydrological models. *Journal of Hydrology*, 466, 1–30.

Thompson, J.R., Green, A.J. and Kingston, D.G., 2014a. Potential evapotranspiration-related uncertainty in climate change impacts on river flow: An assessment for the Mekong River basin. *Journal of Hydrology*, 510, 259–279.

Thompson, J.R. and Hollis, G.E., 1995. Hydrological modelling and the sustainable development of the Hadejia-Nguru Wetlands, Nigeria. *Hydrological Sciences Journal*, 40, 97–116.

Thompson, J.R., Laizé, C.L.R., Green, A.J., Acreman, M.C. and Kingston, D.G., 2014b. Climate change uncertainty in environmental flows for the Mekong River. *Hydrological Sciences Journal*, 59, 259–279.

Thompson, J.R. and Polet, G., 2000. Hydrology and land use in a Sahelian floodplain wetland. *Wetlands*, 20, 639–659.

Thorne, R., 2011. Uncertainty in the impacts of projected climate change on the hydrology of a subarctic environment: Liard River Basin. *Hydrology and Earth System Sciences*, 15, 1483–1492.

Todd, M.C., Taylor, R.G., Osborn, T., Kingston, D., Arnell, N. and Gosling, S., 2011. Uncertainty in climate change impacts on basin-scale freshwater resources – preface to the special issue: the QUEST-GSI methodology and synthesis of results. *Hydrology and Earth System Sciences*, 15, 1035–1046.

Van der Kamp, J., Fofana, B. and Wymenga, E., 2005. Ecological values of the Inner Niger Delta. In: L. Zwarts, P. van Beukering, B. Kone, and E. Wymenga, eds. *The Niger, a lifeline: effective water management in the Upper Niger Basin*. RIZA / Sévaré: Wetlands International / Amsterdam: Institute for Environmental Studies / Veenwouden: A&W Ecological Consultants, 155–176.

Van Dijk, A.I.J.M., Kirby, M., Paydar, Z., Podger, G., Mainuddin, Md., Marvanek, S. and Peña Arancibia, J. 2008. *Uncertainty in river modelling across the Murray-Darling Basin*. A report to the Australian Government from the CSIRO Murray-Darling Basin Sustainable Yields Project, Canberra: CSIRO.

Voinov, A., Costanza, R., Fitz, C. and Maxwell, T., 2007. Patuxent landscape model: 1. hydrological model development. *Water Resources*, 34, 163–170.

Welcomme, R.L., 1986. Fish of the Niger system. In: B.R. Davies and K.F. Walker, eds. *The ecology of river systems*. Dordrecht: Junk, 25–47.

World Bank, United Nations Environment Programme, African Development Bank, French Ministry of Cooperation and European Community, 1993. *Sub-Saharan Africa hydrological assessment*. Washington DC: World Bank.

Xu, H., Taylor, R.G. and Xu, Y. 2011. Quantifying uncertainty in the impacts of climate change on river discharge in sub-catchments of the Yangtze and Yellow River Basins, China. *Hydrology and Earth System Science*, 15, 333–344.

Zhang, L. and Mitsch, W.J., 2005. Modelling hydrological processes in created freshwater wetlands: an integrated system approach. *Environmental Modelling & Software*, 20, 935–946.

Zwarts, L., Cisse, N. and Diallo, M., 2005a. Hydrology of the Upper Niger. In: L. Zwarts, P. van Beukering, B. Kone and E. Wymenga, eds. *The Niger, a lifeline: effective water management in the Upper Niger Basin*. RIZA / Sévaré: Wetlands International / Amsterdam: Institute for Environmental Studies / Veenwouden: A&W Ecological Consultants, 15–41.

Zwarts, L. and Diallo, M., 2005. Fisheries in the Inner Niger Delta. In: L. Zwarts, P. van Beukering, B. Kone and E. Wymenga, eds. *The Niger, a lifeline: effective water management in the Upper Niger Basin*. RIZA / Sévaré: Wetlands International / Amsterdam: Institute for Environmental Studies / Veenwouden: A&W Ecological Consultants, 89–107.

Zwarts, L. and Grigoras, I., 2005. Flooding of the Inner Niger Delta. In: L. Zwarts, P. van Beukering, B. Kone and E. Wymenga, eds. *The Niger, a lifeline: effective water management in the Upper Niger Basin*. RIZA / Sévaré: Wetlands International / Amsterdam: Institute for Environmental Studies / Veenwouden: A&W Ecological Consultants, 43–77.

Zwarts, L., Grigoras, I. and Hanganu, J., 2005b. Vegetation of the lower inundation zone of the Inner Delta. In: L. Zwarts, P. van Beukering, B. Kone and E. Wymenga, eds. *The Niger, a lifeline: effective water management in the Upper Niger Basin*. RIZA / Sévaré: Wetlands International / Amsterdam: Institute for Environmental Studies / Veenwouden: A&W Ecological Consultants, 109–119.

Zwarts, L. and Kone, B., 2005a. People in the Inner Niger Delta. In: L. Zwarts, P. van Beukering, B. Kone, and E. Wymenga, eds. *The Niger, a lifeline: effective water management in the Upper Niger Basin*. RIZA / Sévaré: Wetlands International / Amsterdam: Institute for Environmental Studies / Veenwouden: A&W Ecological Consultants, 79–86.

Zwarts, L. and Kone, B., 2005b. Rice production in the Inner Niger Delta. *In*: L. Zwarts, P. van Beukering, B. Kone and E. Wymenga, eds. *The Niger, a lifeline: effective water management in the Upper Niger Basin*. RIZA / Sévaré: Wetlands International / Amsterdam: Institute for Environmental Studies / Veenwouden: A&W Ecological Consultants, 137–153.

ACCEPTED MANUSCRIPT

Tables

Table 1. GCMs that were pattern-scaled by ClimGen and applied in this study.

GCM	Climate modelling centre and country
CCCMA CGCM3.1	Canadian Centre for Climate Modelling and Analysis (Canada)
CSIRO MK3.0	CSIRO Atmospheric Research (Australia)
IPSL CM4	Institut Pierre Simon Laplace (France)
MPI ECHAM5	Max Planck Institute for Meteorology (Germany)
NCAR CCSM30	National Centre for Atmospheric Research (USA)
UKMO HadGEM1	Hadley Centre for Climate Prediction and Research (UK)
UKMO HadCM3	Hadley Centre for Climate Prediction and Research (UK)

ACCEPTED MANUSCRIPT

Table 2. Model performance statistics for twelve gauging stations within the Upper Niger for the calibration (Cal. 1950–1975), baseline (BL 1961–1990) and validation (Val. 1976–2000) periods. Letters after gauging station names refer to the labels used in Figure 1. Model performance indicators are taken from Henriksen *et al.* (2008).

Station	Period	Data		DV (%) [†]	NSE [*]	r [#]
		availability [†]				
Tinkisso (a)	Cal.	13, 3, 3, 1, 6		-1.44 ☆☆☆☆☆	0.860 ☆☆☆☆☆	0.928
	BL	11, 3, 2, 1, 14		-3.62 ☆☆☆☆☆	0.860 ☆☆☆☆☆	0.928
	Val.	3, 0, 0, 0, 22		4.81 ☆☆☆☆☆	0.790 ☆☆☆☆☆	0.937
Kouroussa (b)	Cal.	14, 5, 6, 1, 0		-1.38 ☆☆☆☆☆	0.846 ☆☆☆☆☆	0.921
	BL	18, 6, 5, 2, 0		-1.65 ☆☆☆☆☆	0.823 ☆☆☆☆☆	0.908
	Val.	13, 4, 6, 2, 0		10.53 ☆☆☆	0.765 ☆☆☆☆☆	0.899
Banankoro (c)	Cal.	5, 3, 0, 1, 17		-5.46 ☆☆☆☆☆	0.928 ☆☆☆☆☆	0.965
	BL	13, 4, 5, 1, 8		0.10 ☆☆☆☆☆	0.925 ☆☆☆☆☆	0.962
	Val.	13, 4, 6, 1, 1		11.87 ☆☆☆	0.898 ☆☆☆☆☆	0.961
Kankan (d)	Cal.	24, 1, 1, 0, 0		-4.95 ☆☆☆☆☆	0.857 ☆☆☆☆☆	0.936
	BL	25, 5, 1, 0, 0		-3.01 ☆☆☆☆☆	0.897 ☆☆☆☆☆	0.954
	Val.	13, 11, 1, 0, 0		3.46 ☆☆☆☆☆	0.863 ☆☆☆☆☆	0.940
Sankarani (e)	Cal.	9, 2, 1, 0, 14		-3.83 ☆☆☆☆☆	0.863 ☆☆☆☆☆	0.931
	BL	12, 4, 3, 0, 12		-3.05 ☆☆☆☆☆	0.835 ☆☆☆☆☆	0.916
	Val.	4, 2, 2, 0, 17		-0.60 ☆☆☆☆☆	0.688 ☆☆☆☆☆	0.840
Bougouni (f)	Cal.	13, 5, 1, 0, 7		-5.00 ☆☆☆☆☆	0.876 ☆☆☆☆☆	0.943
	BL	18, 4, 0, 0, 9		-5.22 ☆☆☆☆☆	0.861 ☆☆☆☆☆	0.933
	Val.	8, 0, 0, 0, 17		-5.19 ☆☆☆☆☆	0.878 ☆☆☆☆☆	0.937
Pankourou (g)	Cal.	7, 11, 2, 0, 6		-4.97 ☆☆☆☆☆	0.862 ☆☆☆☆☆	0.932
	BL	10, 12, 1, 0, 8		-5.31 ☆☆☆☆☆	0.839 ☆☆☆☆☆	0.921
	Val.	6, 2, 0, 0, 17		-2.52 ☆☆☆☆☆	0.819 ☆☆☆☆☆	0.918
Koulikoro (h)	Cal.	26, 0, 0, 0, 0		-3.65 ☆☆☆☆☆	0.948 ☆☆☆☆☆	0.974
	BL	31, 0, 0, 0, 0		-0.34 ☆☆☆☆☆	0.932 ☆☆☆☆☆	0.965
	Val.	24, 1, 0, 0, 0		11.41 ☆☆☆	0.879 ☆☆☆☆☆	0.961
Douna (i)	Cal.	15, 5, 6, 0, 0		-9.75 ☆☆☆☆☆	0.907 ☆☆☆☆☆	0.956
	BL	24, 3, 4, 0, 0		-4.26 ☆☆☆☆☆	0.882 ☆☆☆☆☆	0.940
	Val.	22, 1, 2, 0, 0		16.32 ☆☆☆	0.721 ☆☆☆☆☆	0.925
Ke-Macina (j)	Cal.	16, 3, 4, 0, 3		0.01 ☆☆☆☆☆	0.954 ☆☆☆☆☆	0.980
	BL	16, 4, 4, 0, 7		1.33 ☆☆☆☆☆	0.936 ☆☆☆☆☆	0.971
	Val.	7, 2, 0, 0, 16		12.35 ☆☆☆	0.874 ☆☆☆☆☆	0.956
Beney-Kegny (k)	Cal.	16, 5, 4, 0, 1		-6.78 ☆☆☆☆☆	0.897 ☆☆☆☆☆	0.953
	BL	15, 4, 4, 0, 8		-9.39 ☆☆☆☆☆	0.864 ☆☆☆☆☆	0.936
	Val.	7, 0, 1, 0, 17		-9.50 ☆☆☆☆☆	0.770 ☆☆☆☆☆	0.883
Dire (l)	Cal.	24, 2, 0, 0, 0		-4.81 ☆☆☆☆☆	0.901 ☆☆☆☆☆	0.952
	BL	28, 3, 0, 0, 0		4.64 ☆☆☆☆☆	0.853 ☆☆☆☆☆	0.942
	Val.	20, 3, 1, 0, 1		17.81 ☆☆☆	0.685 ☆☆☆☆☆	0.893
Performance indicator	Excellent ☆☆☆☆☆	Very good ☆☆☆☆	Fair ☆☆☆	Poor ☆☆	Very poor ☆	
Dv	< 5%	5–10%	10–20%	20–40%	>40%	
NSE	>0.85	0.65–0.85	0.50–0.65	0.20–0.50	<0.20	

† number of years during the calibration, validation or baseline periods for which 12, 9–11, 5–8, 1–4 and 0 months of discharge data are available, + bias (Henriksen *et al.*, 2003), * Nash-Sutcliffe coefficient (Nash and Sutcliffe, 1970), # Pearson correlation coefficient.

Table 3. Mean annual precipitation (Precip.) and potential evapotranspiration (PET) for the baseline (mm) and changes (%) for the climate change scenarios for sub-catchments within the Upper Niger catchment. (Shaded cells indicate negative changes compared to the baseline).

		Sub-catchments (letters refer to model sub-catchments indicated in Figure 1)											
Parameter	Scenario	a	b	c	d	e	f	g	h	i	j	k	l
Precip.	Baseline	1384.3	1677.0	1564.1	1730.2	1457.5	1282.6	1198.7	1056.3	957.8	585.2	740.7	446.1
	CCCMA	-7.7	-5.9	-5.8	-5.8	-5.6	-5.8	-5.4	-4.1	-2.7	-2.7	0.0	0.7
	CSIRO	-1.4	2.3	4.9	6.2	4.3	2.9	-0.5	-2.1	-4.8	-5.9	-5.2	-1.6
	HadCM3	-3.2	1.4	0.5	2.8	2.3	2.1	2.2	-2.2	-0.8	-6.6	3.6	-1.7
	HadGEM1	-8.6	-9.2	-6.7	-9.0	-5.3	-1.8	-1.2	-1.7	0.5	1.5	2.4	7.1
	IPSL	-31.5	-30.0	-25.9	-22.2	-17.9	-17.0	-16.1	-18.6	-5.5	-18.0	-13.2	-10.2
	MPI	-7.0	-4.0	-3.8	-2.8	-2.2	-1.6	-1.0	-6.3	-4.3	-11.9	-6.3	-11.1
	NCAR	-2.4	0.5	-0.8	0.0	0.0	0.6	1.0	-1.9	1.0	4.0	7.4	14.4
PET	Baseline	1883.9	1856.4	1920.7	1908.5	1924.3	1922.6	1924.1	1968.1	1969.7	2043.8	2015.3	2089.9
	CCCMA	6.5	5.7	5.8	5.5	5.6	5.5	5.3	6.1	5.8	5.9	5.6	5.2
	CSIRO	5.8	5.3	5.5	5.1	5.3	5.4	5.4	6.0	6.0	6.0	6.2	5.9
	HadCM3	6.4	5.8	6.3	6.2	6.7	7.0	7.0	7.2	7.3	7.4	7.3	7.0
	HadGEM1	3.4	3.1	3.3	3.0	2.9	2.7	2.2	2.8	2.4	2.8	2.6	2.9
	IPSL	6.7	6.3	6.4	6.2	6.3	6.3	6.1	6.4	6.2	6.1	6.1	5.6
	MPI	6.9	6.4	6.5	6.2	6.2	6.1	5.8	6.7	6.3	6.7	6.5	6.1
	NCAR	2.8	2.0	2.4	2.1	2.4	2.5	2.6	3.4	3.5	4.5	4.2	3.8

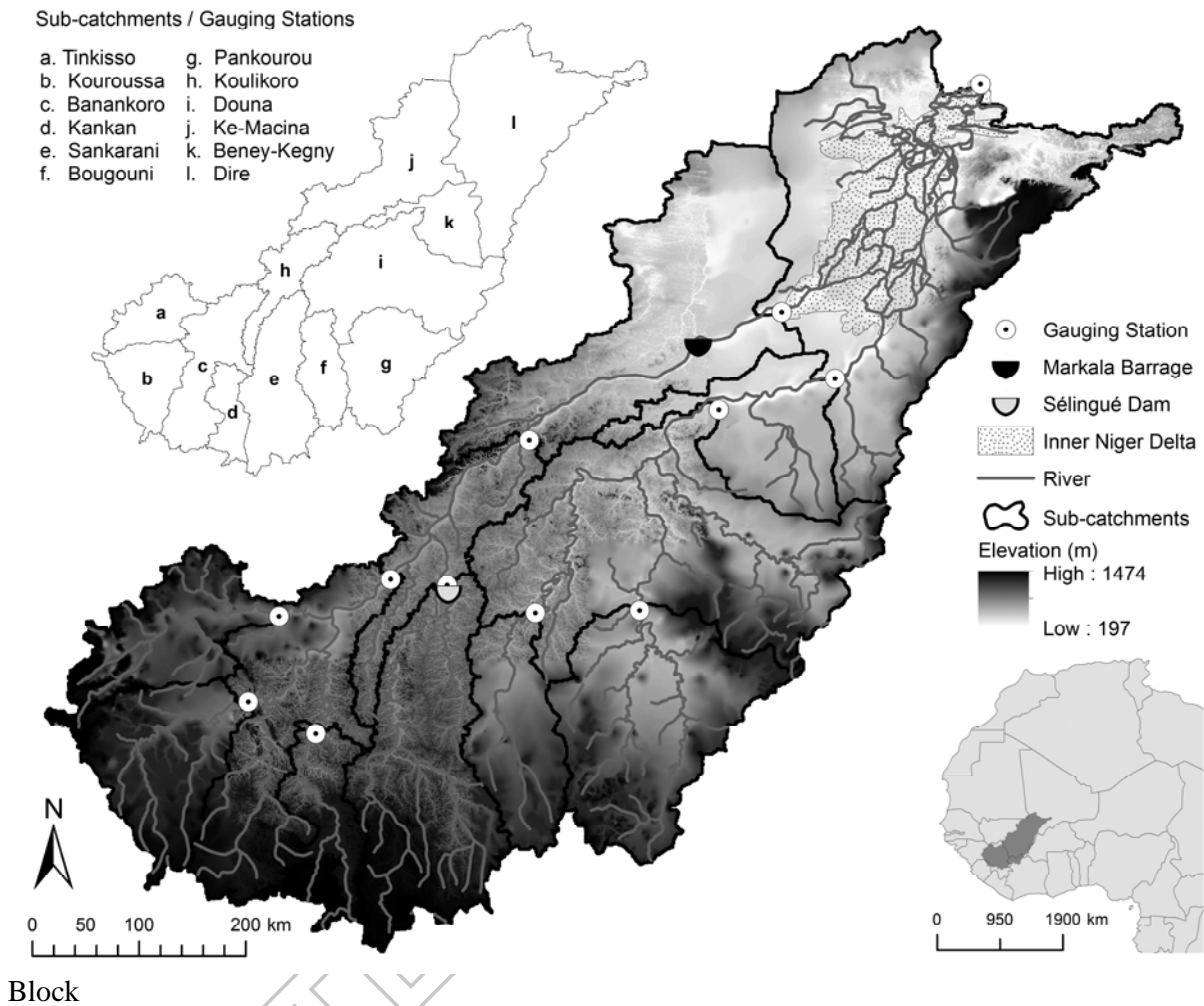
Table 4. Mean annual mean, Q5 and Q95 discharges for the baseline (m^3s^{-1}) and changes (%) for the climate change scenarios for 12 gauging stations within the Upper Niger catchment. (Shaded cells indicate negative changes compared to the baseline).

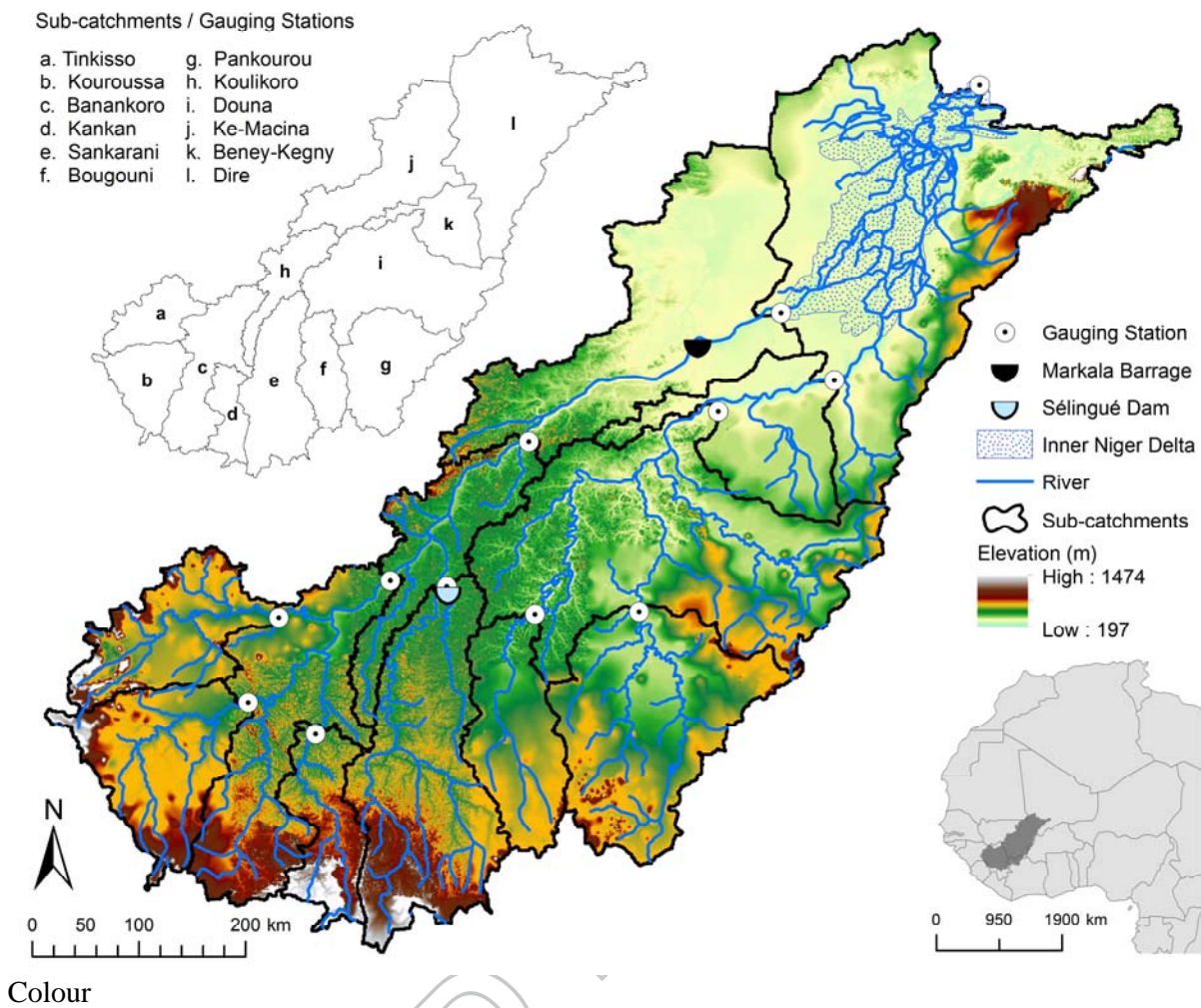
Parameter	Scenario	Gauging station (letters refer to gauging stations indicated in Figure 1)											
		a	b	c	d	e	f	g	h	i	j	k	l
Mean	Baseline	138.8	194.6	924.3	163.4	299.7	86.8	164.2	1235.2	340.9	1171.2	344.8	928.8
	CCCMA	-29.0	-22.5	-23.3	-23.3	-21.0	-34.2	-33.9	-23.1	-33.1	-24.2	-32.7	-18.3
	CSIRO	-8.9	-2.5	3.1	10.8	5.5	-3.5	-17.5	3.2	-21.6	3.0	-21.1	-0.8
	HadCM3	-8.4	3.3	0.9	3.6	1.2	-0.7	-1.7	0.7	-6.1	0.6	-5.7	-1.5
	HadGEM1	-12.2	-12.4	-5.5	-2.7	8.6	22.2	23.3	-1.8	22.2	-1.5	22.0	0.3
	IPSL	-68.4	-56.7	-52.9	-45.5	-37.0	-53.9	-54.0	-49.7	-57.0	-51.8	-55.8	-42.5
	MPI	-14.3	-7.5	-6.3	-2.5	1.7	2.8	3.7	-4.6	-1.2	-4.7	-1.1	-4.0
	NCAR	-17.9	-9.1	-14.3	-16.2	-15.8	-24.5	-23.9	-15.1	-25.9	-15.9	-25.5	-11.9
Q5	Baseline	593.9	712.5	3602.2	624.5	1160.2	416.9	919.2	4726.2	1730.0	4709.5	1742.0	2128.7
	CCCMA	-22.6	-14.3	-16.0	-16.9	-17.5	-29.3	-28.4	-17.5	-26.2	-20.8	-25.5	-7.2
	CSIRO	-2.7	1.8	3.4	9.9	0.9	-5.5	-15.7	4.3	-16.2	0.3	-19.1	-1.4
	HadCM3	-2.8	6.0	2.8	7.5	2.1	0.4	-0.1	3.5	-6.8	2.5	-4.0	-0.4
	HadGEM1	-3.2	-0.1	2.8	6.2	14.0	21.3	17.1	4.0	21.3	0.2	16.7	1.4
	IPSL	-53.1	-42.2	38.7	30.8	28.9	-42.6	-44.2	-38.0	-47.1	-40.2	-46.1	-16.8
	MPI	-6.8	1.2	0.9	5.2	4.4	-2.1	3.7	0.0	-0.8	-1.7	0.8	-1.4
	NCAR	-15.9	-6.8	-10.2	-9.4	-12.9	-20.7	-20.1	-12.7	-19.6	-14.2	-18.8	-5.0
Q95	Baseline	0.6	3.4	8.0	1.5	0.2	0.1	0.1	10.3	0.5	0.0	0.8	0.0
	CCCMA	-50.0	-32.4	-30.0	-26.7	-50.0	-100.0	-100.0	-37.9	-100.0	-†	-75.0	-†
	CSIRO	0.0	-11.8	16.3	6.7	0.0	0.0	-100.0	-2.9	-80.0	-†	-62.5	-†
	HadCM3	16.7	-5.9	2.5	0.0	0.0	0.0	0.0	-14.6	-60.0	-†	-37.5	-†
	HadGEM1	-16.7	-32.4	-15.0	-13.3	-50.0	0.0	0.0	-26.2	80.0	-†	150.0	-†
	IPSL	-83.3	-67.6	-63.8	-46.7	-50.0	-100.0	-100.0	-67.0	-100.0	-†	-75.0	-†
	MPI	-33.3	-14.7	-12.5	-6.7	-50.0	0.0	-100.0	-21.4	-60.0	-†	-37.5	-†
	NCAR	0.0	-17.6	-15.0	-20.0	-50.0	-100.0	-100.0	-20.4	-100.0	-†	-75.0	-†

† Baseline and scenario Q95 = 0 m^3s^{-1} .

Figure Captions

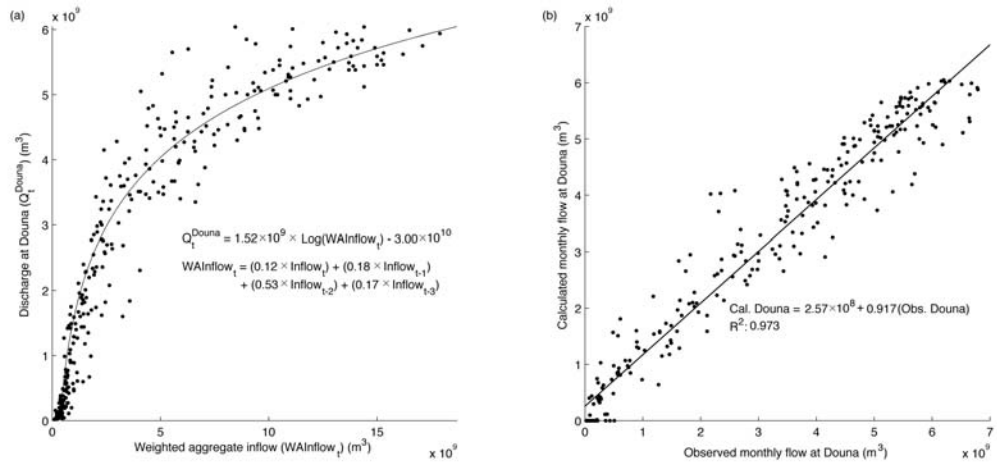
Figure 1. The Upper Niger Catchment and the Inner Niger Delta. The sub-catchments and their downstream gauging stations for which separate sub-models were developed are indicated.





ACCEPTED

Figure 2. (a) The relationship between weighted aggregate inflow to the Inner Niger Delta (Ke-Macina + Beney-Kegny) and monthly outflow (Douna), (b) comparison between observed and calculated monthly flows at Douna. Analyses are based on the period 1953–1992 using GRDC gauging station records.



ACCEPTED MANUSCRIPT

Figure 3. Monthly mean observed and simulated discharges for seven gauging stations within the Upper Niger for the period 1950–2000. The calibration (1950–1975), validation (1976–2000) and baseline (1961–1990) periods are indicated. Note different y-axis scales. Letters in brackets refer to the sub-catchments identified in Figure 1.

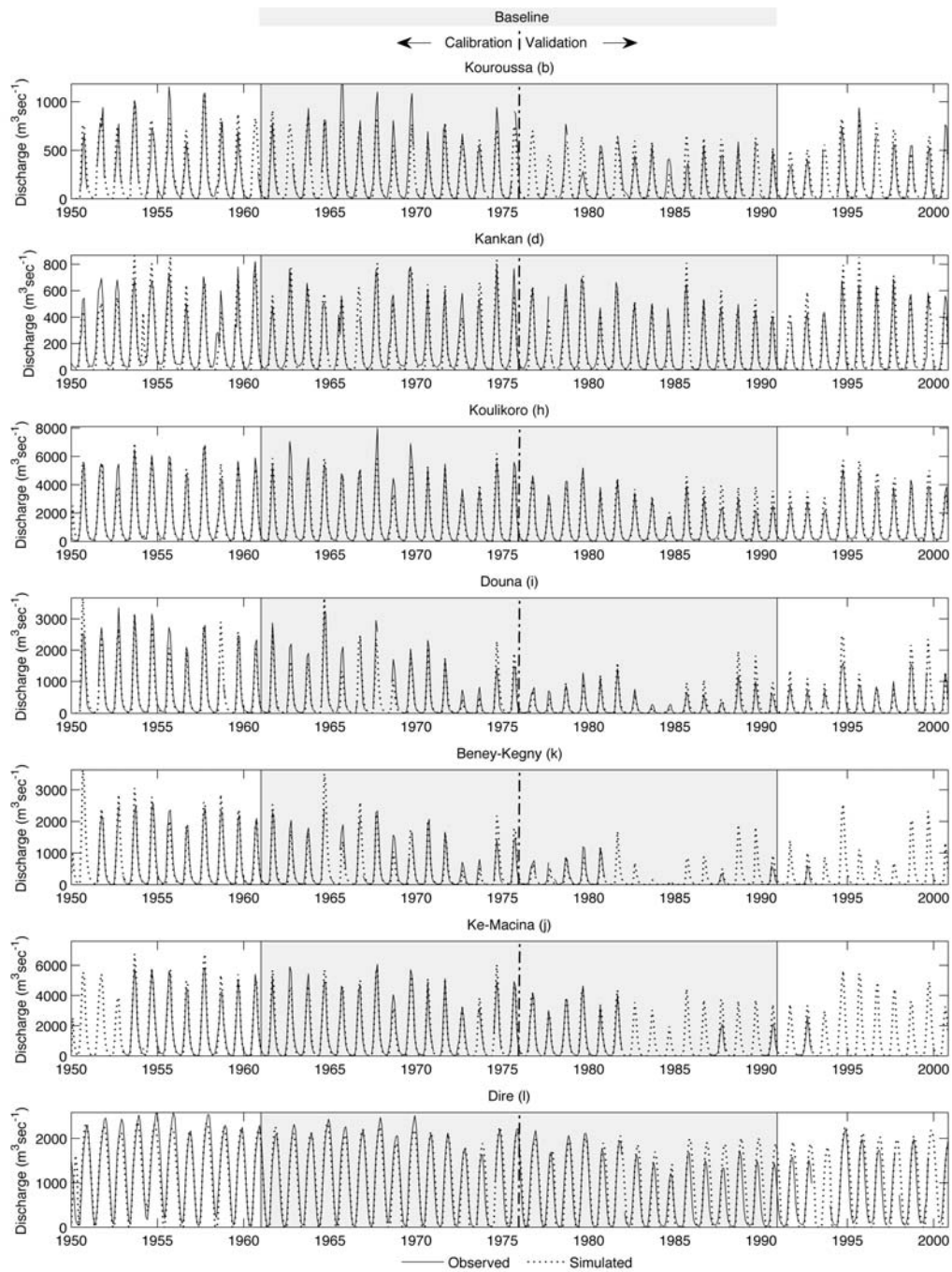


Figure 4. Observed and simulated mean monthly discharges for 12 gauging stations within the Upper Niger for the period for the calibration (1950–1975), baseline (1961–1990) and validation (1976–2000) periods. Note different y-axis scales. Letters in brackets refer to the sub-catchments identified in Figure 1. Symbols in square brackets indicate availability for each period: + Good, +- Medium, - Poor.

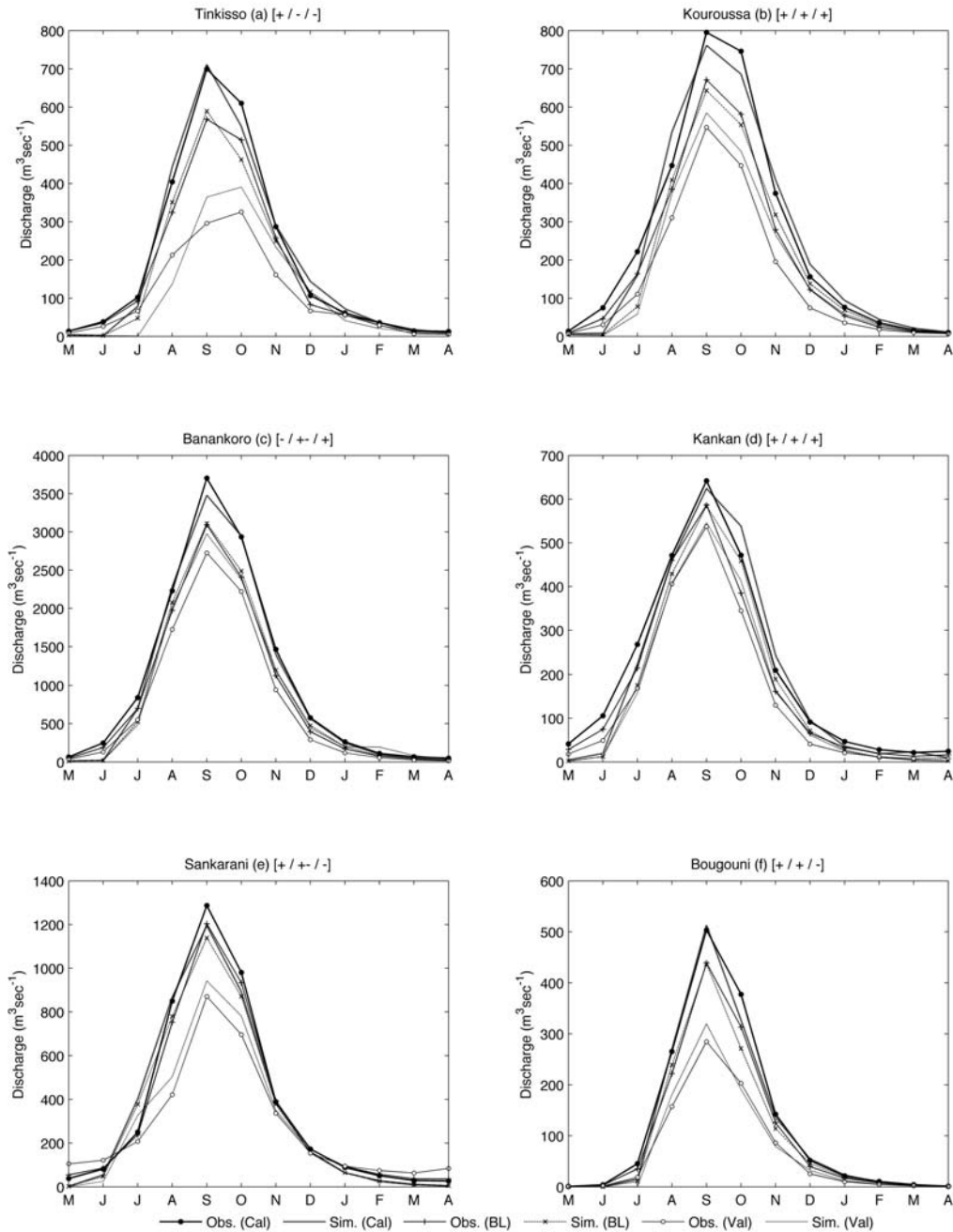


Figure 4 Part a

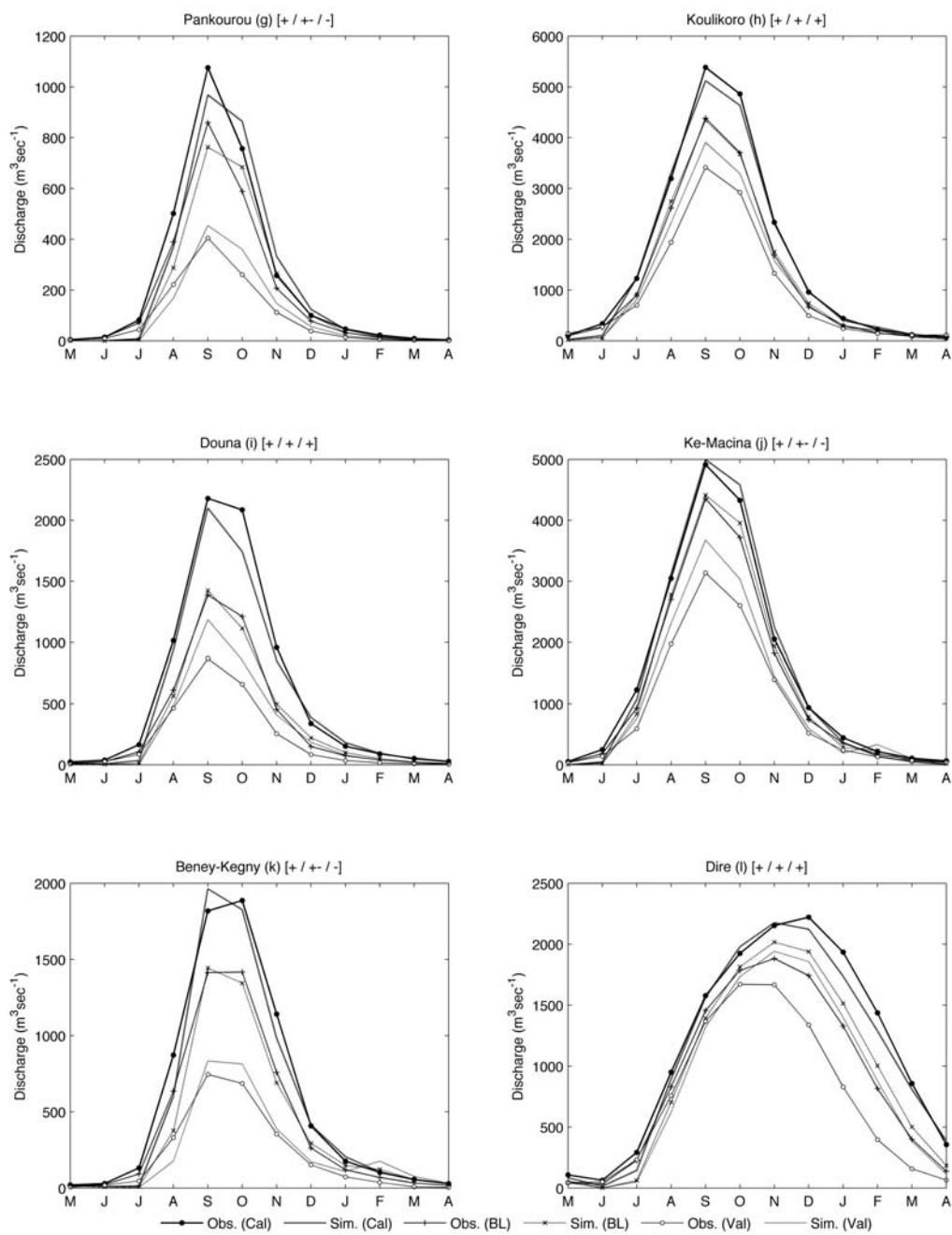
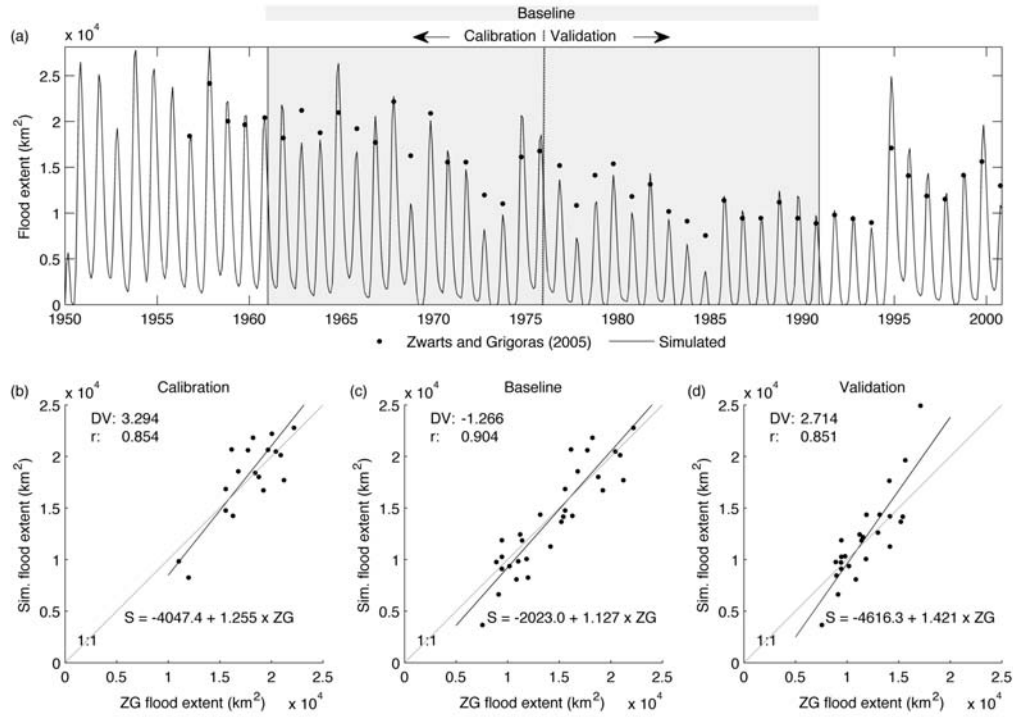


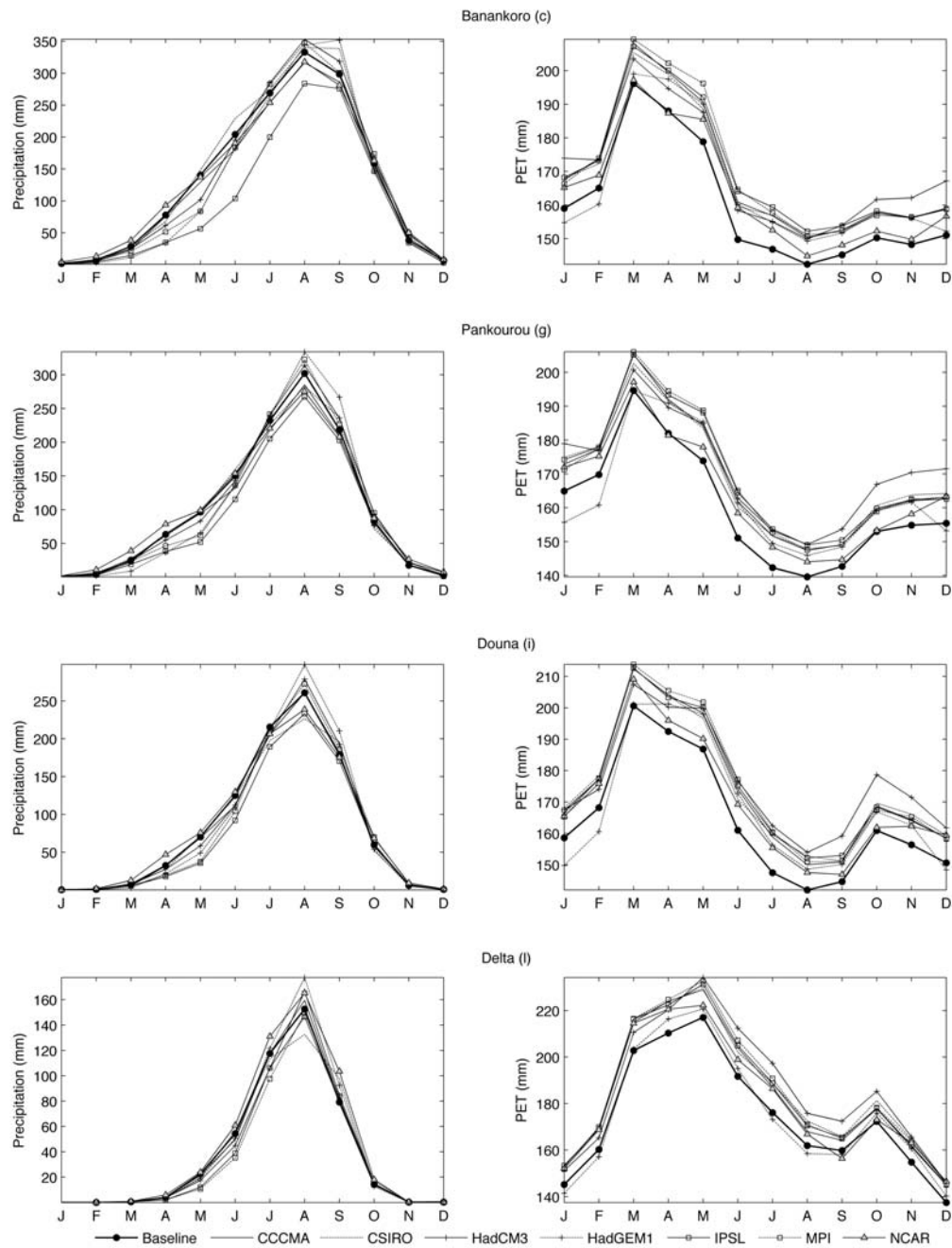
Figure 4 Part b

Figure 5. Flood extent within the Inner Niger Delta: (a) simulated monthly flood extent and annual maxima provided by Zwarts and Grigoras (2005); (b, c, d) simulated (S) vs Zwarts and Grigoras (2005) (ZG) annual maximum flood extents for the calibration, baseline and validation periods, respectively.



ACCEPTED MANUSCRIPT

Figure 6. Mean monthly precipitation and PET for the baseline and the 2 °C, seven GCM climate change scenarios for four representative sub-catchments within the Upper Niger. Note different y-axis scales. Letters in brackets refer to the sub-catchments identified in Figure 1.



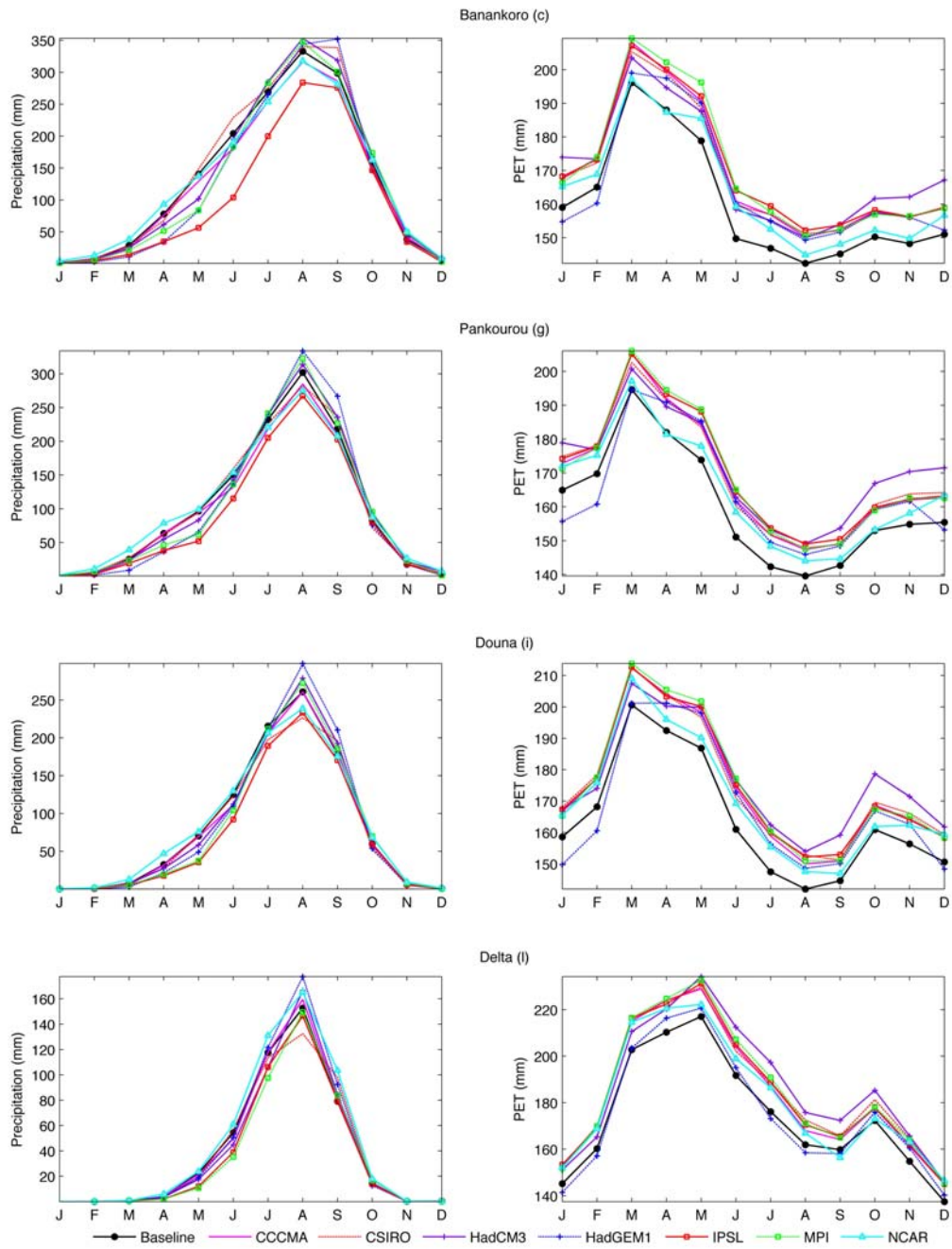
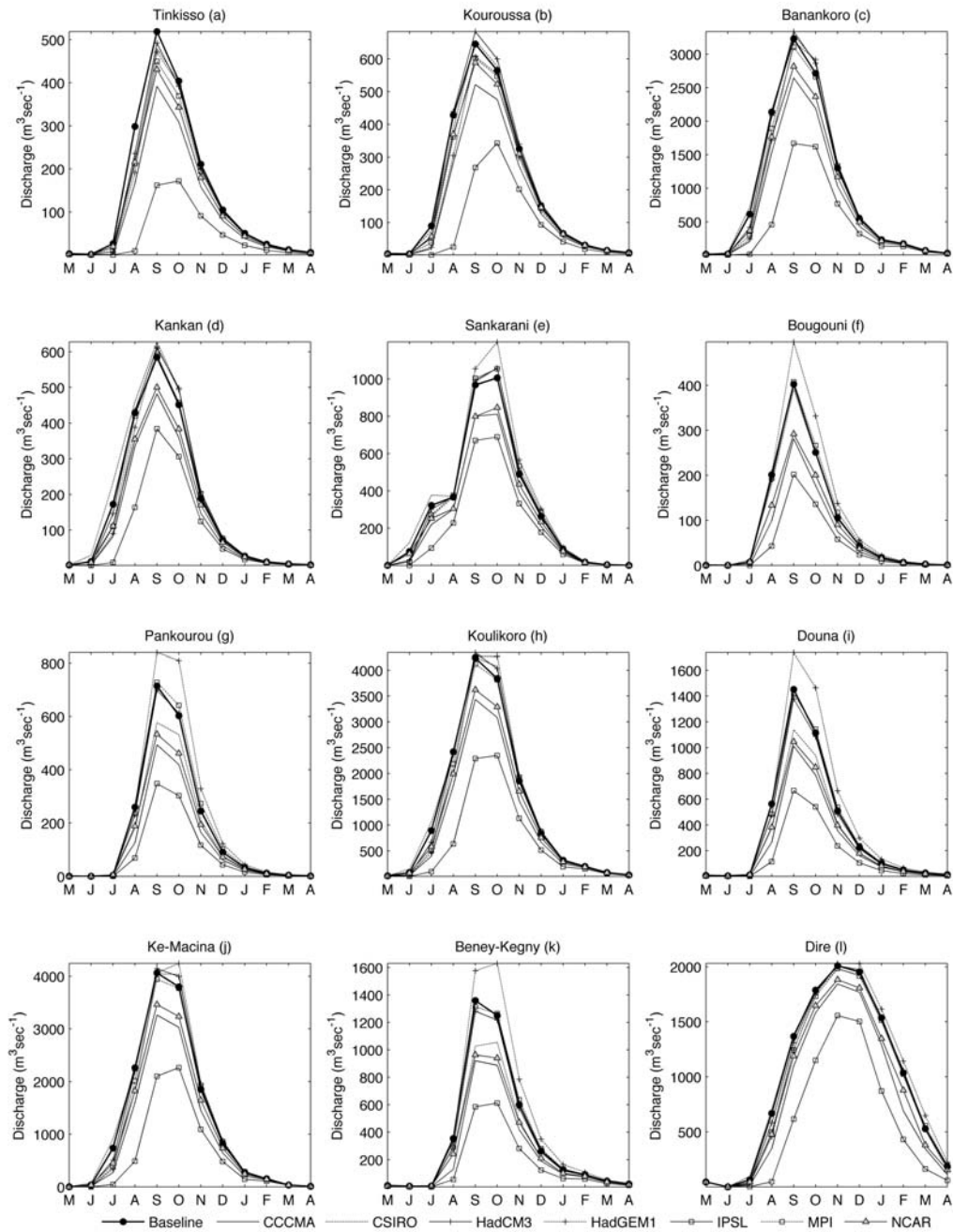


Figure 7. Simulated river regimes for the baseline and 2 °C, seven GCM climate change scenarios for 12 gauging stations within the Upper Niger. Note different y-axis scales. Letters in brackets refer to the sub-catchments identified in Figure 1.



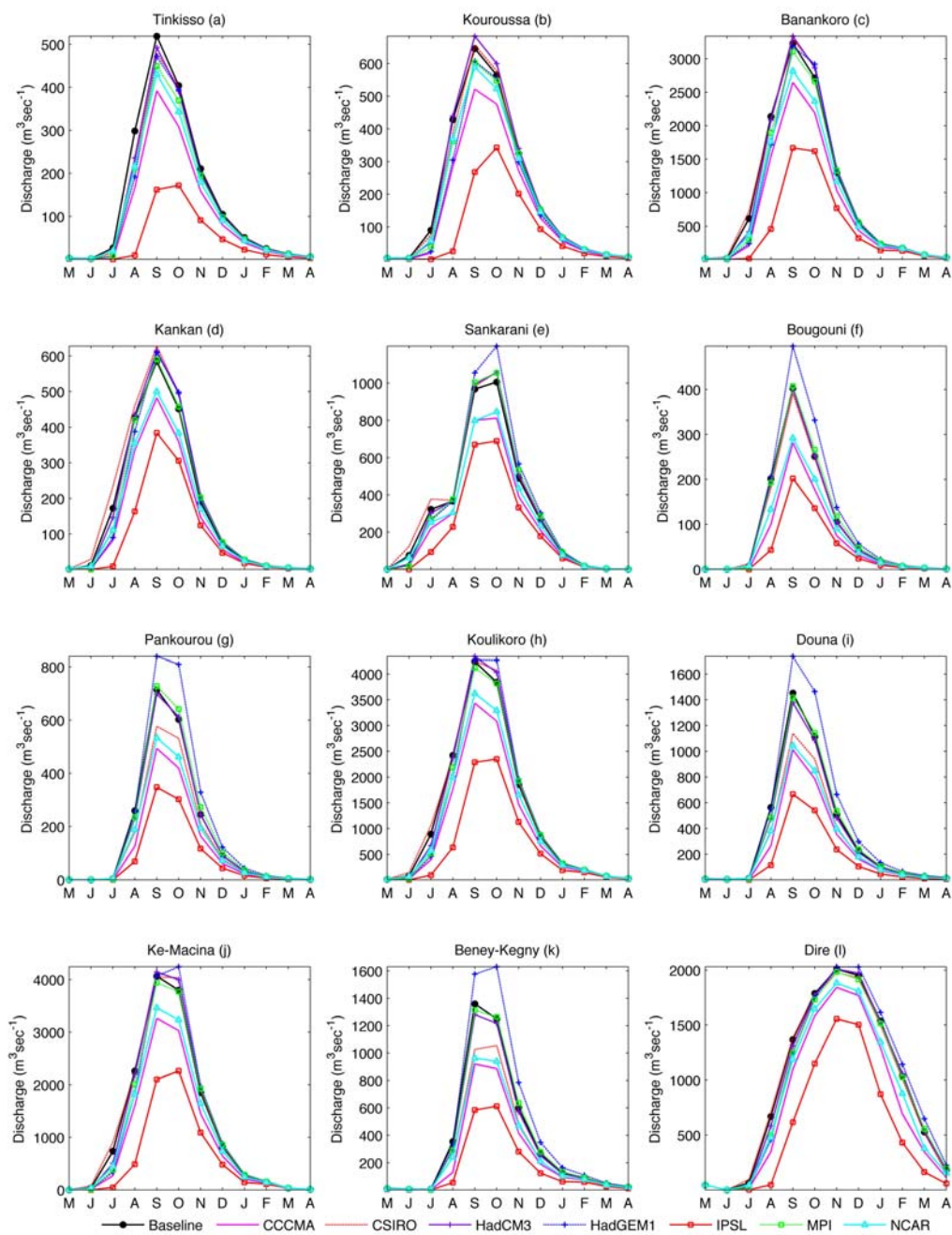
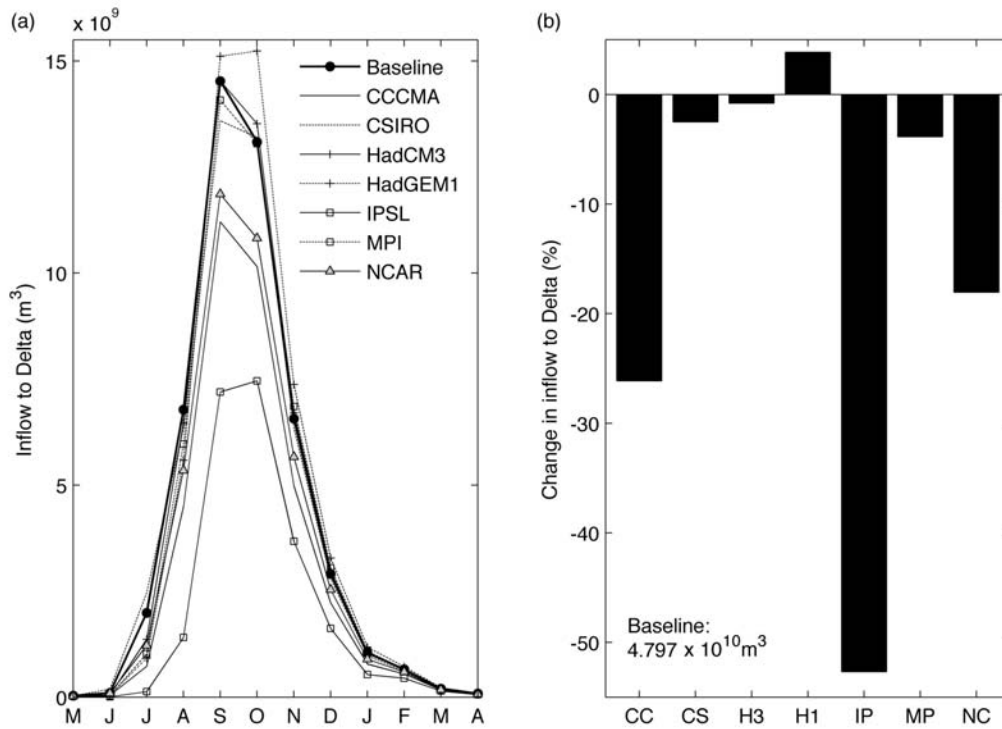
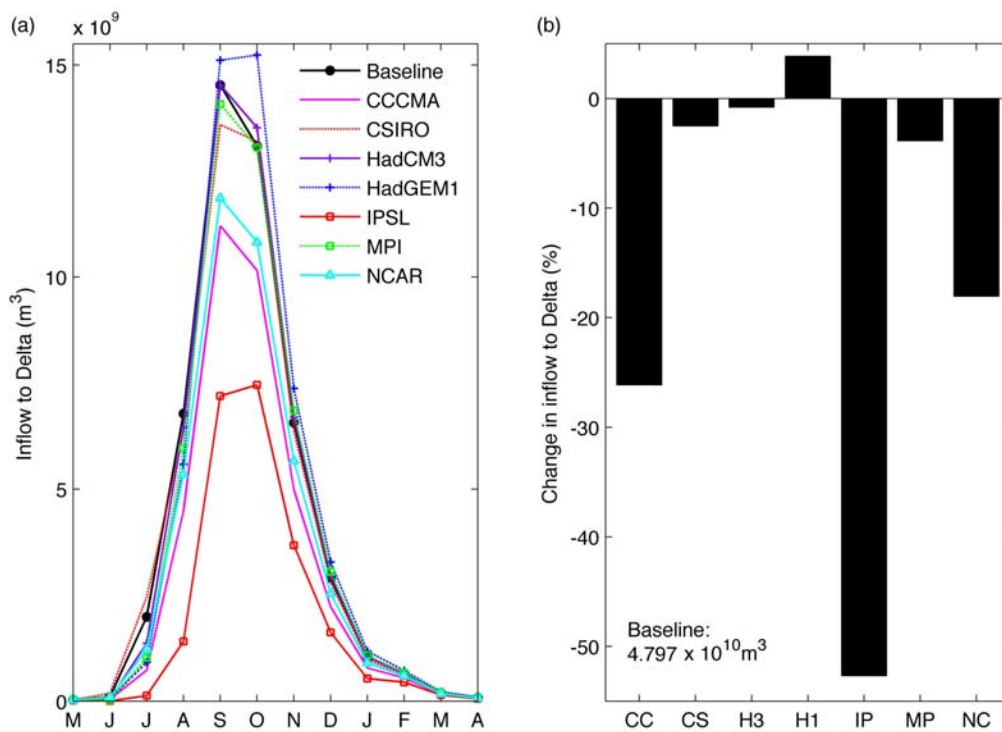


Figure 8. Baseline and 2 °C, seven GCM climate change scenario river inflows to the Inner Niger Delta: (a) mean monthly inflows; (b) scenario change in mean annual inflows compared to the baseline. CC = CCCMA; CS = CSIRO; H3 = HadCM3; H1 = HadGEM1; IP = IPSL; MP = MPI; NC = NCAR.



Block



Colour

Figure 9. Flood regimes for the Inner Niger Delta for the baseline and 2 °C, seven GCM climate change scenarios.

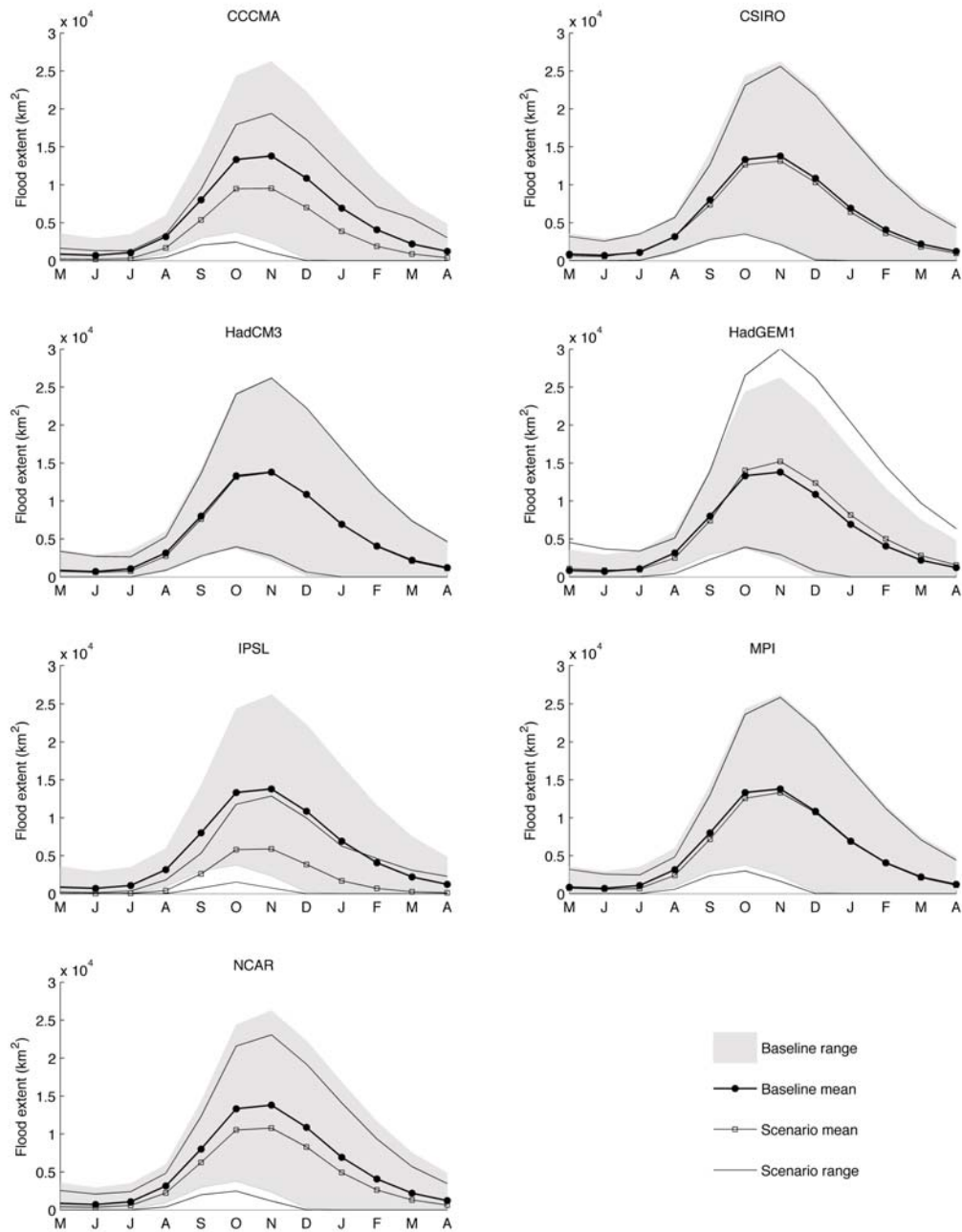
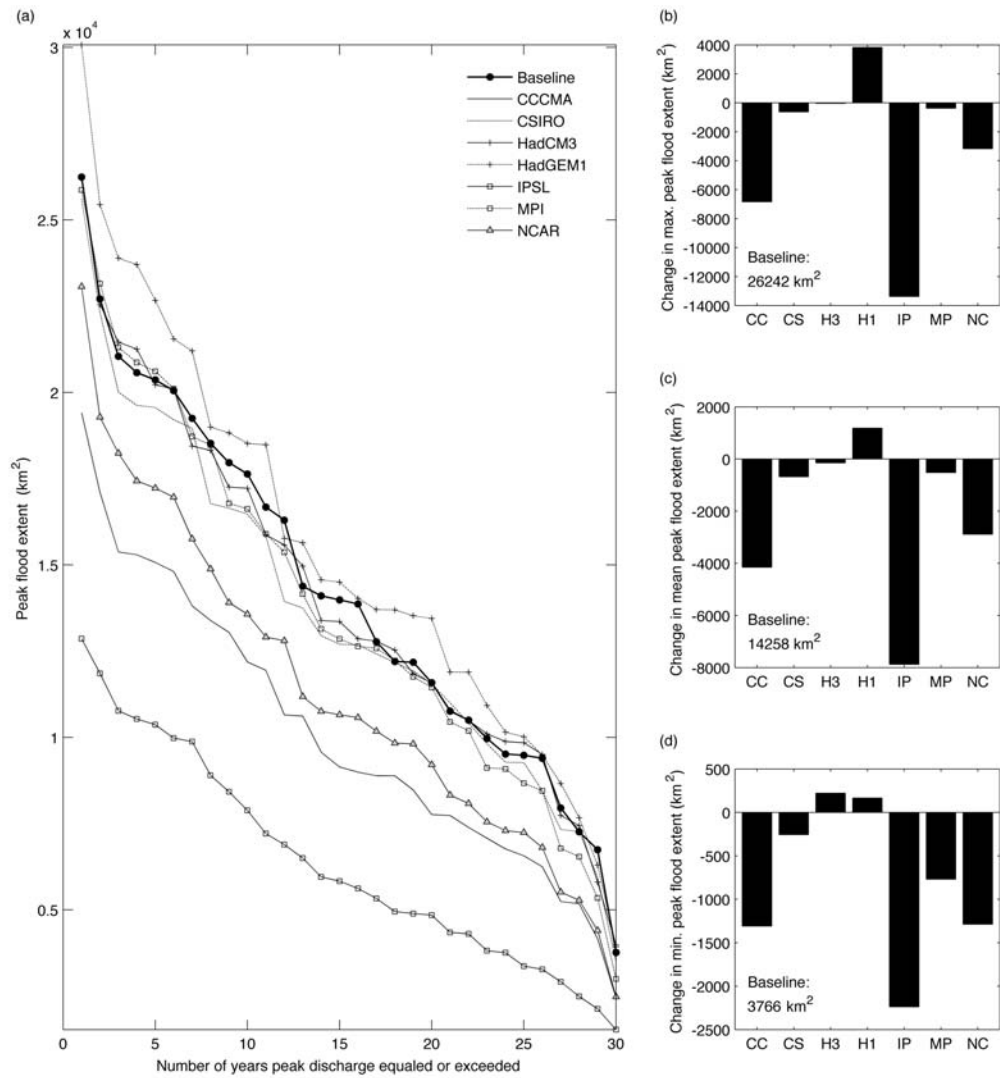
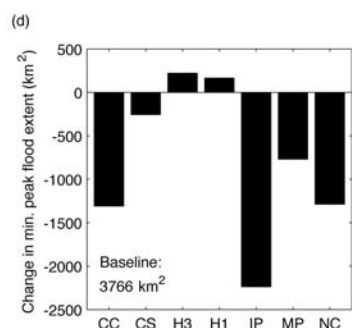
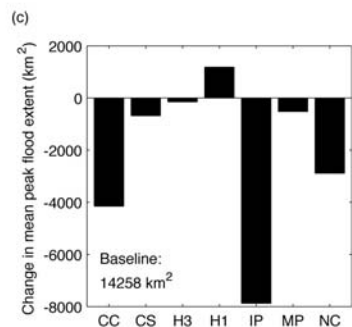
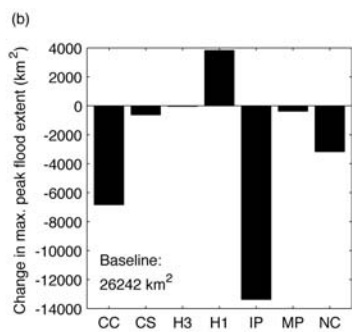
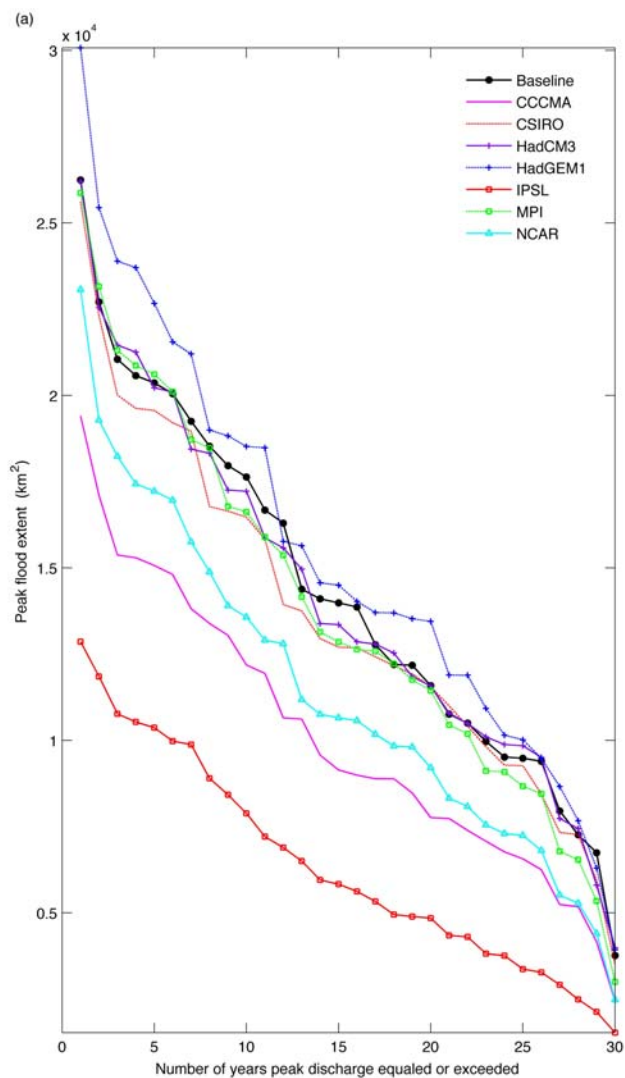


Figure 10. Impacts of the 2 °C, seven GCM climate change scenarios on annual peak flood extents within the Inner Niger Delta: (a) peak flood extent-frequency for the baseline and each scenario; (b-d) change from the baseline in the maximum, mean and minimum annual peak flood extents. CC = CCCMA; CS = CSIRO; H3 = HadCM3; H1 = HadGEM1; IP = IPSL; MP = MPI; NC = NCAR.



Block



Colour

ACCEPTED